Volume 5
Number 10
December 2020
Pages 1549–1708

MSDE

Molecular Systems Design & Engineering

rsc.li/molecular-engineering

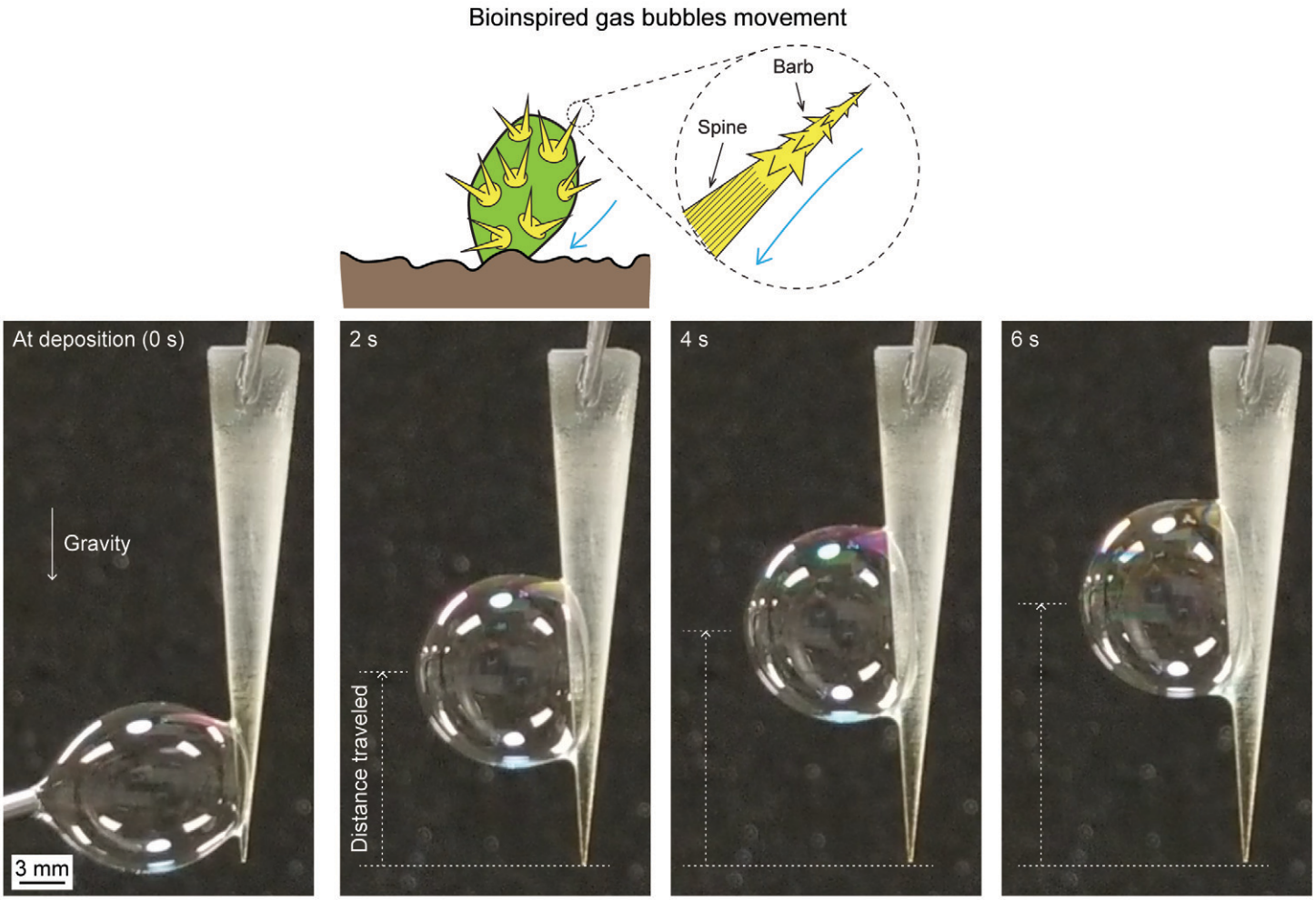

ISSN 2058-9689

ROYAL SOCIETY OF CHEMISTRY

REVIEW ARTICLE

Dev Gurera and Bharat Bhushan

Bioinspired movement of gas bubbles: composition, applications, generation, contact angle, and movement – an overview

IChemE ADVANCING CHEMICAL ENGINEERING WORLDWIDE

MSDE

REVIEW

View Article Online
View Journal | View Issue

Cite this: *Mol. Syst. Des. Eng.*, 2020, **5**, 1555

Bioinspired movement of gas bubbles: composition, applications, generation, contact angle, and movement – an overview

Dev Gurera and Bharat Bhushan *

Received 24th July 2020,
Accepted 9th September 2020

DOI: 10.1039/d0me00099j

rsc.li/molecular-engineering

Gas bubbles are of interest in various applications including biomedicine, food production, drag reduction, water treatment, oil removal and surface cleaning. Therefore, studying gas bubbles in its entirety and their movement is important. In this paper, an overview is presented on gas bubbles in terms of their composition, applications, generation, and contact angles, with focus on their movement on bioinspired conical surfaces and triangular patterns. Effects of parameters including gas bubble volume, orientation, tip angle, surface wettability, and liquid were also presented.

Design, System, Application

Bioinspiration is an emerging field of study. It involves the understanding of biological functions, structures, and principles of various objects found in Nature by biologists, physicists, chemists, materials scientists, and engineers, and can lead to the biologically inspired design, adaptation, or derivation from living Nature. Since the early 2000s, there have been significant advances in research using bioinspiration, and many ideas are commercialized in areas including oil-water separation, self-healing, fluid-drag reduction, bio- and inorganic fouling, dry adhesion, structural coloration, and painless piercing. Along the same line, this paper is aimed at advancing bioinspired gas bubble movement. Gas bubbles are of interest in various applications including biomedicine, food production, drag reduction, water treatment, oil removal and surface cleaning. Therefore, studying gas bubbles in its entirety and their movement is important. Inspiration for moving gas bubbles mainly comes from cacti and spider web. They provide inspiration for designing conical surfaces and triangular patterns, which create a Laplace pressure gradient inside the gas bubbles which helps in their movement. The Laplace pressure gradient can also move the gas bubbles against gravity or buoyancy.

Nanoprobe Laboratory for Bio- & Nanotechnology and Biomimetics (NLBB), The Ohio State University, 201 W. 19th Avenue, Columbus, Ohio 43210-1142, USA. E-mail: bhushan.2@osu.edu

Dev Gurera

Dev Gurera is a PhD student at The Ohio State University (OSU), USA, in the department of Mechanical Engineering, working with Prof. Bhushan. Dev's research is focused on finding bioinspired solutions to modern problems. Which includes: painless microneedle; self-cleaning and less-sticky synthetic leather; water harvesting from moisture; gas bubbles movement. He is an experimentalist by training. Broadly, he has worked on topics including coatings, micro–/nanostructures, surface roughness, and wettability. He also holds a Master of Science from OSU, and a Bachelor of Technology from Indian Institute of Technology (IIT) Ropar, India; both majoring in mechanical engineering.

Bharat Bhushan

Dr. Bharat Bhushan is an Ohio Eminent Scholar and Howard D. Winbigler Professor, and Director of Nanoprobe Laboratory for Bio- & Nanotechnology and Biomimetics (NLBB) at Ohio State University. His research interests include scanning probe techniques in bio/nanotribology, bio/nanomechanics and bio/nanomaterials characterization and applications to bio/nanotechnology and biomimetics. He has authored 10 books and 900+ papers and edited more than 50 books. He holds 25 US and foreign patents. He is one of the top 1500 highly cited researchers in the world in all fields, with an h-index of 130+ with 80 k+ citations.

1 Introduction

Gas bubbles are of interest in various applications including biomedicine, food production, drag reduction, water treatment, oil removal and surface cleaning.[1–6] For example, in the field of biomedicine, gas bubbles are used as contrast agents in biomedical imaging and have been explored for drug delivery and as anti-inflammatory agents for therapeutic intervention in neuroinflammatory or neurodegenerative disorders.[1,7,8] In the field of food production, gas bubbles help in improving functional and aromatic components of food and beverages.[9,10] Gas bubbles also help in drag reduction *via* changing density, viscosity, and compressibility of the flowing liquid.[11] In the field of environment, gas bubbles help in wastewater treatment, by its decomposition and oil removal or degreasing.[12–14] On the contrary, gas bubbles may also have a deleterious effect. For example, the gas bubbles produced in oil, including carbon dioxide–hydrogen sulfide and oxygen, could potentially cause corrosion of pipelines resulting in reduced equipment life and wasted resources.[15] Therefore, the study of gas bubbles movement in terms of their formation, interaction with underlying surfaces, and their movement is important.

The gas bubbles based on its composition can be broadly divided into two categories: in air and under liquid. Fig. 1 shows schematics of the various gas bubbles' composition. In-air gas bubble is a gas enclosed by a thin liquid film. These gas bubbles are typically present in air, therefore the term "in air" is been used. These gas bubbles surely can be present in other gases as well. A typical example of such gas bubbles is a soap bubble.[16–18] The under-liquid gas bubbles have comparatively more common occurrence.[4] These are gas bubbles under a liquid. A few examples of liquids include water, hexadecane, and soap + water solution.[19] For both compositions of gas bubbles, various examples of enclosed gases include air, oxygen, nitrogen, and carbon dioxide.

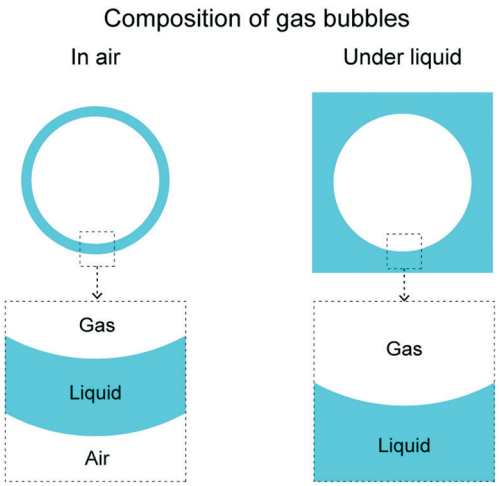

Fig. 1 Composition of various gas bubbles. Gas bubbles can be broadly divided into two categories: in air and under liquid.

There are various forces which help in gas bubbles movement. As an example, for in-air gas bubbles, there is always gravity acting downwards. A gas bubble with high mass will experience high force. As another example, for under-liquid gas bubbles, there is buoyancy force acting upwards. A gas bubble with high volume and/or high density of surrounding liquid will experience high force. However, forces like these have their limitations. The direction of these kind of forces cannot be controlled and the force magnitude can be negligible for low volume or low mass gas bubbles, such as nanobubbles and microbubbles.

Inspiration for developing a more efficient way of moving the gas bubbles comes from cacti and spider web. Both the species have a curvature gradient in their surfaces, on which a collected water droplet always move from a higher curvature area to a lower curvature area.[20] The curvature gradient creates a Laplace pressure gradient inside which drives it towards lower curvature. Based on this mechanism, bioinspired conical surfaces and triangular patterns have been developed and extensively used for collecting and moving water droplets. In which a water droplet always moves away from the tip, towards the base. Similarly, bioinspired conical surfaces and bioinspired triangular pattern have also been developed and studied for gas bubbles movement.[17–19,21,22] Both types of gas bubbles, in air and under liquid, have been studied.

In this paper, an overview is presented on various aspects of gas bubbles keeping their bioinspired movement as the primary focus. These various aspects as summarized as following. First, an overview on presented on the bioinspiration, cacti and spider web, and the mechanism using which a gas bubble is moved. Next, various applications of gas bubbles are presented, including biomedicine, food production, drag reduction, water treatment, oil removal and surface cleaning. Next, various methods of gas bubbles generation are presented, including use of outer liquid flow fields and acoustic forcing. Next, contact angles of gas bubbles on surfaces with various wettabilities is presented. Next, the bioinspired gas bubble movement is discussed using conical surfaces and triangular patterns. The movement is discussed by varying parameters including gas bubble volume, cone/triangle orientation, tip angle, surface wettability, and liquids used.

2 Bioinspiration for gas bubbles movement: cacti and spider web

Inspiration for efficient and controlled movement of gas bubbles comes from cacti and spider web.

Both the species have been studied for moving collected water droplets.[20] The water droplets get collected on their surface due to fog and/or condensation of water vapors. The water droplets move because of their evolved surface structures. The mechanism for water droplet movement used by cacti and spider web have been shown schematically in Fig. 2(a) and 3(a), respectively. The water droplet movement

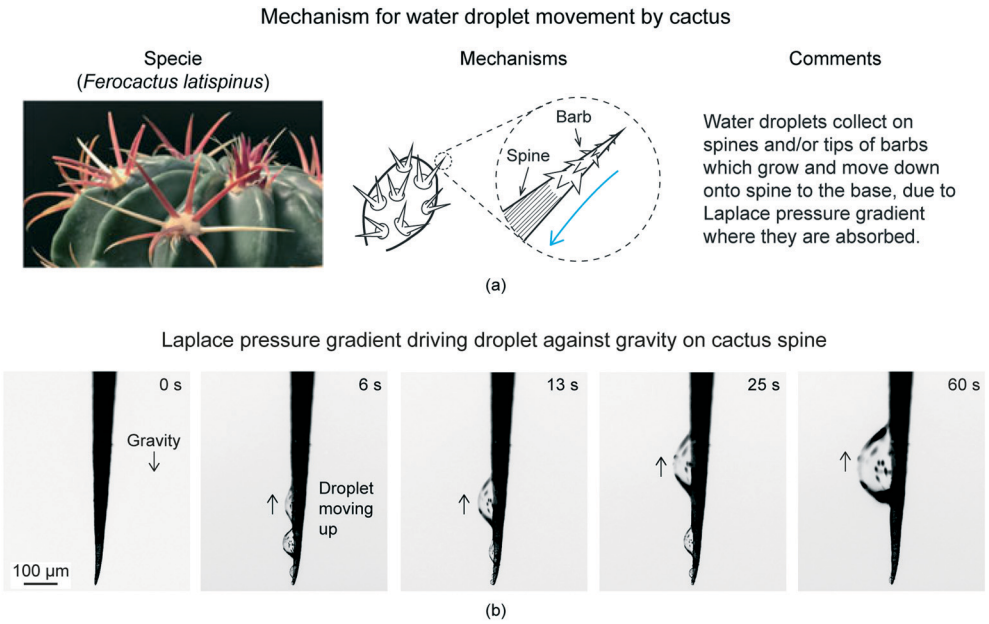

Fig. 2 (a) Mechanism used by cactus to move water droplets (adapted from ref. 25). (b) Optical images of water droplets initially collected at the barb tip and/or spines of *Ferocactus latispinus*, climbed up over the cactus spine due to Laplace pressure gradient (adapted from ref. 25). Droplets defy gravity.

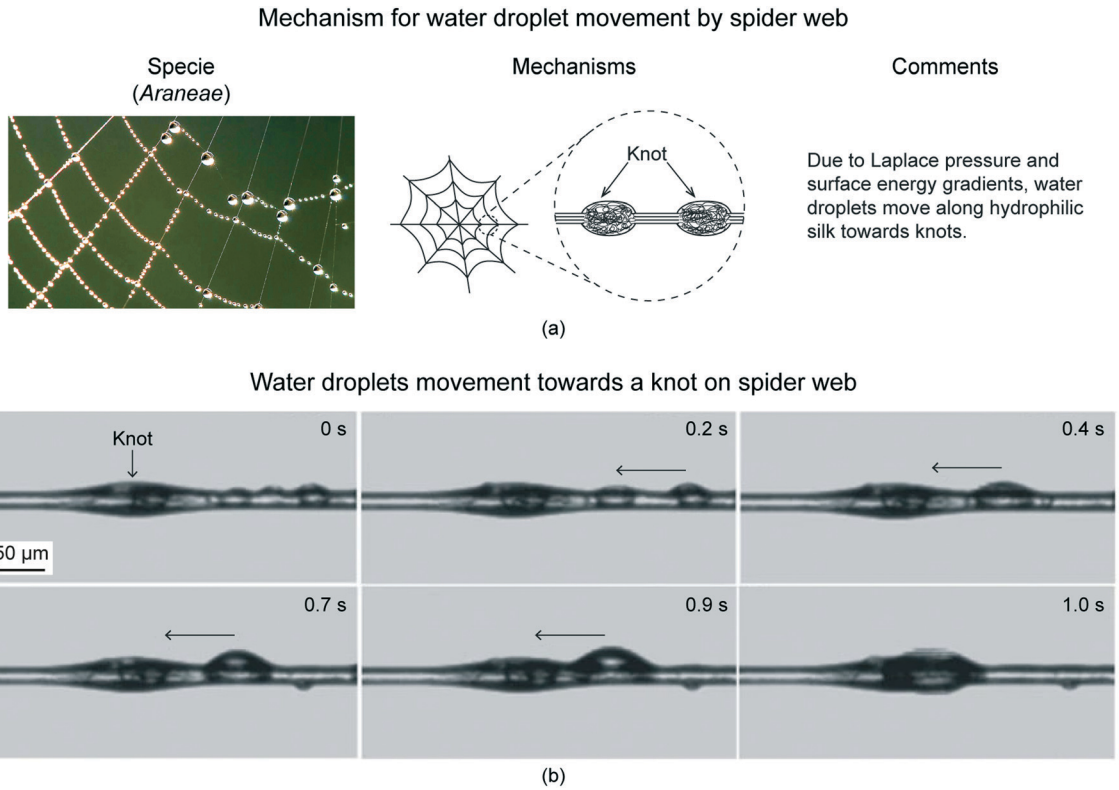

Fig. 3 (a) Mechanism used by spider silk to move water droplets (adapted from ref. 25). (b) Optical images showing preferential transport of water droplets towards knots on a spider web (adapted from ref. 24).

used by cacti and spider web have been shown using optical images in Fig. 2(b) and 3(b), respectively. Cactus has conical spines with microscopic conical barbs on it, as shown in Fig. 2(a) for *Ferocactus latispinus* specie.[20,23] Water droplets collect on the conical spine and move towards the base due to curvature gradient providing Laplace pressure gradient. Droplets may also collect on the tips of the small barbs and once they reach critical size, they move onto the conical spine. Once at the base of the spine, the plant absorbs the water. Laplace pressure gradient is large enough such that water droplets can defy gravity and climb upward, as shown in Fig. 2(b). Similar can also be applied for spider web. Spider web has a "beads on a string" structure with a series of knots periodically spaced along the silk thread, shown in Fig. 3(a) for *Araneae* specie.[20] The knots have rougher surface as compared to the silk thread's surface. When water collects on the spider web, the droplets are found to move toward the knots, as shown in Fig. 3(b).[20,23,24] A combination of a surface tension gradient and a Laplace pressure gradient is believed to be responsible for the water movement. Surface tension gradient occurs due to the knots displaying a rougher surface. The roughness enhances their hydrophilicity. Laplace pressure gradient occurs due to the curvature gradient. Droplets, therefore, move on a conical fiber from regions of smaller radius to regions of larger radius.

Similar strategy can be applied for gas bubbles movement on conical surfaces and triangular patterns. As an example for conical surfaces, an under-liquid gas bubble sitting on a constant curvature surface has a constant Laplace pressure of

$$\Delta P = 2\gamma/(r + h) \quad (1)$$

where γ is the surface tension of the liquid, r is the radius of the curvature of the underlying surface, and h is the height of the gas from the centerline.[6,20,26] As a curvature gradient is introduced in the underlying surface, there is a resultant Laplace pressure gradient introduced inside the gas bubble. The resultant Laplace pressure gradient results in a gas bubble moving toward regions of a larger radius, as it will decrease the average Laplace pressure inside the gas bubble. This means that a gas bubble moves away from the tip on a conical surface.[18,19] As another example for triangular patterns, for an under-liquid gas bubble constrained between two boundaries of a triangular pattern has a local Laplace pressure of

$$\Delta P \sim 2\gamma \sin\theta(x)/w(x) \quad (2)$$

where γ is the surface tension of the liquid, x is distance from tip of the triangle, $\theta(x)$ is contact angle at the boundaries, and $w(x)$ is the local width of the triangle at a distance x.[20] The two ends of the gas bubble will have different widths, which will generate a Laplace gradient inside the gas bubble. The resultant Laplace pressure gradient results in a gas bubble moving toward regions of a larger width, as it will decrease the average Laplace pressure inside the gas bubble. This means a gas bubble will move from away from the tip on a triangular pattern. For in-air gas bubble, the pressure will be twice as shown in the above two equations because it has two interfaces instead of one, as shown in Fig. 1.

3 Applications of gas bubbles

In this section, various applications of gas bubbles are discussed in detail. First, biomedicine applications are discussed, followed by food production, drag reduction, water treatment, oil removal and surface cleaning.

3.1 Biomedicine

Gas bubbles are widely used as therapeutics and diagnostics for a wide variety of biomedicine applications. The unique ability of gas bubbles to respond to ultrasound makes them useful agents for contrast ultrasound imaging, molecular imaging, and targeted drug and gene delivery.[1,2,7] The gas bubbles used for biomedicine applications are under-liquid gas bubbles with a shell. The shell acts as a stabilizer to the gas bubble, drug carrier, and selective binder to receptor. Fig. 4(a) shows schematic of the biomedicine applications' gas bubble.[2] The diameter of a gas bubble is approximately equal to the size of a red blood cell (about 10 μm diameter), which allows it to display similar rheology in the microvessels and capillaries throughout the body. The gas core comprises most of the particle volume and provides the mechanism for ultrasound backscatter and drug delivery. An example of gases used is perfluorocarbon.

Gas bubbles of this size in aqueous media are inherently unstable owing to surface tension effects,[28] and therefore require a stabilizing shell.[2] The shell typically comprise of surfactants, lipids, proteins, polymers, or a combination of these materials.[2] Thickness of these shells are about 1–200 nm. Drugs can be loaded on the gas bubble shell, embedded in the shell matrix, or loaded in the internal void.[27] Fig. 4(b) shows selected examples of drug loading strategies. The drugs can be loaded on the shell of gas bubbles, embedded in the shell matrix, or loaded in the internal void. For lipid-shelled gas bubbles, the drug can be inserted in the lipid shell, in a thick oil layer underneath the lipid shell, on a positively charged shell through electrostatic force, or bonded to the shell *via* a biotin–avidin bridging system. For protein- or polymer-shelled gas bubbles, the drug can be entrapped in the thick cross-linked protein or polymer matrix, or loaded in the internal void.

The surface of gas bubbles can further be functionalized with ligands that specifically bind to receptors at the target region, thereby increasing focal gas bubble attachment and local drug concentration. Upon disruption of gas bubbles by ultrasound, a high dose of drugs is released only in the sonicated region. Fig. 5(a) shows schematics of gas bubbles attaching to target sites and drug release on application of external ultrasound.[27] This system allows for non-invasive targeted release of drugs while minimizing systemic toxicity to the rest of the body, making it a highly beneficial drug

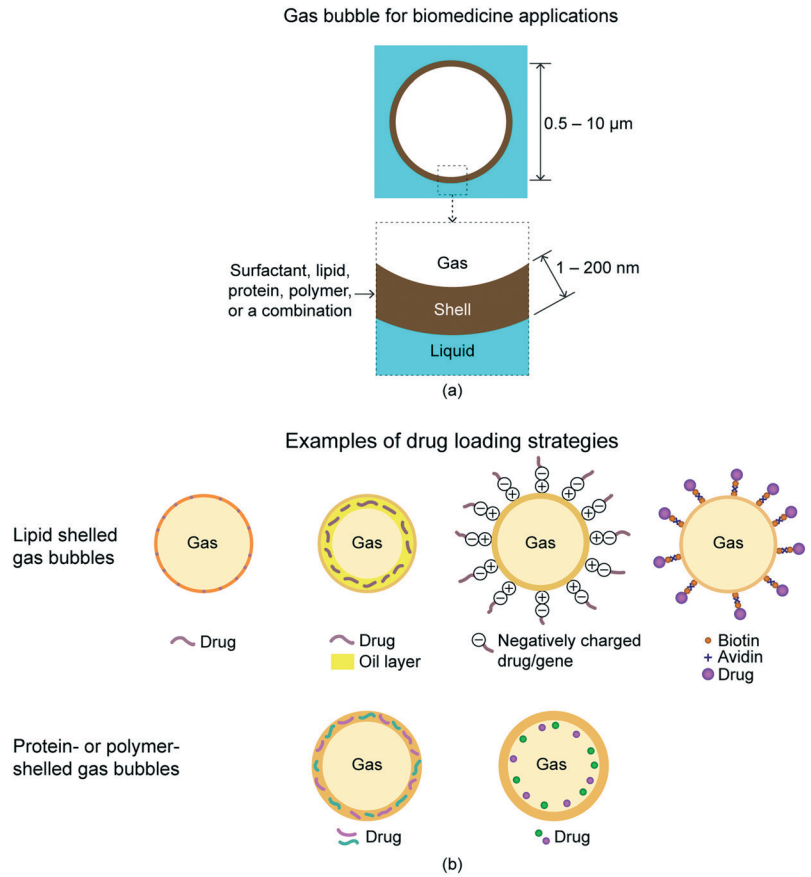

Fig. 4 (a) There is a subcategory of under-liquid gas bubbles with a shell, which is for biomedicine applications.[2] (b) Examples of drug loading strategies.[27] The drugs can be loaded on the shell of gas bubbles, embedded in the shell matrix, or loaded in the internal void.

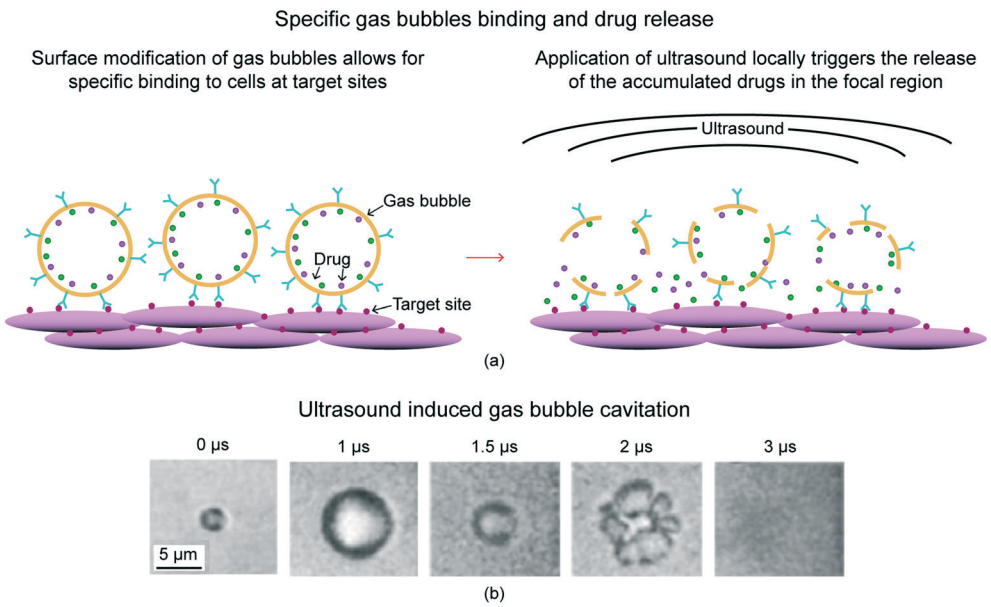

Fig. 5 (a) Schematic of gas bubbles' specific binding and drug release.[27] Surface modification of gas bubbles allows for specific binding to cells at target sites, increasing local drug concentration. Application of ultrasound locally triggers the release of the accumulated drugs in the focal region. (b) Cavitation of gas bubbles under ultrasound using optical images (adapted from ref. 29). Gas bubbles undergo volumetric expansion, contraction, fragmentation, and coalesce in response to the ultrasound.

delivery system. When gas bubbles are exposed to the alternating compressional and rarefractional phases of ultrasound, they undergo volumetric expansion, contraction, fragmentation, and coalesce, a process called cavitation. Fig. 5(b) shows gas bubble different steps of cavitation at various times using optical images.[29]

For imaging, high frequencies of ultrasound are needed to make the gas bubbles vibrate particularly strongly.[30] This makes them several thousand times more reflective than normal body tissues. In this way they enhance both grey scale images and flow mediated Doppler signals. As well as being useful in itself, the resonance that gas bubbles produce has several special properties that can be exploited to improve diagnoses. Just as with a musical instrument, multiple harmonic signals, or overtones, are produced. Ultrasound scanners can be tuned to "listen" to these harmonics, producing strong preferential imaging of the gas bubbles in an image.

3.2 Food production

Use of gas bubbles in food is generally termed as aeration.[4,9,10] Owing to their visual appeal and sensory perception, gas bubbles have been attracting consumer attention in foods for quite some time. In food, incorporation of gas bubbles in food reduces the density of the product. Foams could well be a replacer of many commodities responsible for obesity, such as fat, that acts primarily as a flavor and perception enhancer. Entrapment of large amounts of air in the form of steam or water also could provide a means of lowering the calorific value of food. Ice cream is a well-known confectionary among all ages that contains a mixture of milk proteins, polysaccharides, salt, ice-crystals, and gas bubbles. Reportedly, air can be incorporated in ice cream up to 50% of its volume, whereas the minimum incorporation possible is at 10–15%. Incorporation of air in such an emulsified matrix provides a stable gas volume and a pleasant mouthfeel. Such an aerated product concomitantly yields a better texture and appearance that attracts consumers, and thereby increases market demand for aerated products.

In beverages and liquids, gas bubbles or foam or froth is a hallmark of many liquid foods and beverages such as carbonated soft drinks, beer, wine, cappuccino coffee, whipped cream, and ice cream. Incorporation of air in beverages is reported to improve the body and acceptability.[9,10] Despite the favorable effect on appearance, aeration could also risk oxidation in beverages. The air entrapped in the liquid column could initiate spoilage and flavor loss upon prolonged storage.

3.3 Drag reduction

By injection air through small holes on a surface of a ship advancing in water, the frictional drag can be reduced.[4,11] This phenomenon is called air lubrication drag reduction, and research is going on for its application as a clean energy-saving device suited to ships. Gas bubbles formed through injection on ships are on the order of 0.5 mm to 1 mm, and they tend to grow larger by coalescence in downstream. If enough gas is injected beneath a flat surface, the bubbles may coalesce to form a gas layer. There are various mechanisms behind the drag reduction.[11] First, the presence of the gas changes the average density and viscosity of the fluid. Second, the gas bubbles may interact with the turbulent flow of the liquid to modify the turbulent transport. Third, the gas bubbles introduce compressibility to the flow. And, fourth, the dynamics and interactions of the gas bubbles (*e.g.*, splitting and coalescence) may lead to changes in the flow.

3.4 Water treatment

Introducing gas bubbles into water helps in purifying water.[12,31] The process is commonly known as aeration. Aeration water treatment is effective for management of dissolved gases such as radon, carbon dioxide, some taste and odor problems such as methane, and hydrogen sulfide, as well as volatile organic compounds, or industrial solvents. It is also effective in precipitating dissolved iron and manganese. Aeration raises the pH of water.

Aeration treatment consists of passing large amounts of air through water and then venting the air outside. The air causes the dissolved gases or volatile compounds to release from the water. The air and the contaminants released from the water are vented. In the case of iron and manganese, the air causes these minerals to move from their dissolved state to a solid state and precipitate out of solution. The water can then move through a filter to trap the iron and manganese particles.

A similar aeration is used in aquaculture. Aeration helps in maintaining adequate level of oxygen and cleaning water.[32,33]

3.5 Oil removal (degreasing)

In electronics manufacturing for semiconductors, liquid crystal displays and fine-structured equipment, the cleaning process is one of the most important processes to determine the qualities of the materials and products.[4] In some cases, it occupies a third of the total process. In fine-structured equipment manufacturing, in order to remove industrial grease (degreasing) used for cutting metals, the annual amount of 100 000 tons of volatile organic compounds, acidic and alkaline solvents, are consumed. To reduce that, technology for oil removal using gas bubbles has been developed. Fig. 6 compares mechanisms for oil removal using detergents and gas bubbles.[34] One of the biggest problems with oil removal using detergents is the disability in separating the oil from the detergent solution due to the high affinity of the detergent solution and oil. However, using gas bubbles, the oil gets attached to the gas bubble as an outer layer. The gas bubble eventually rises up to the surface and bursts. The floating oil can then be manually

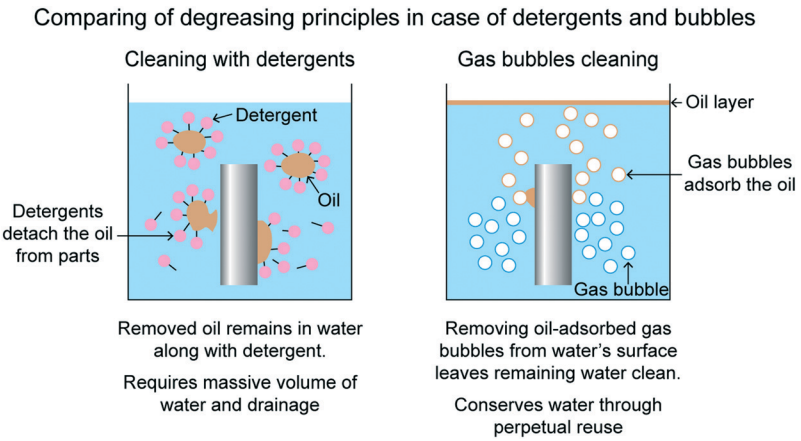

Fig. 6 Comparing of degreasing principles in case of detergents and bubbles.[34]

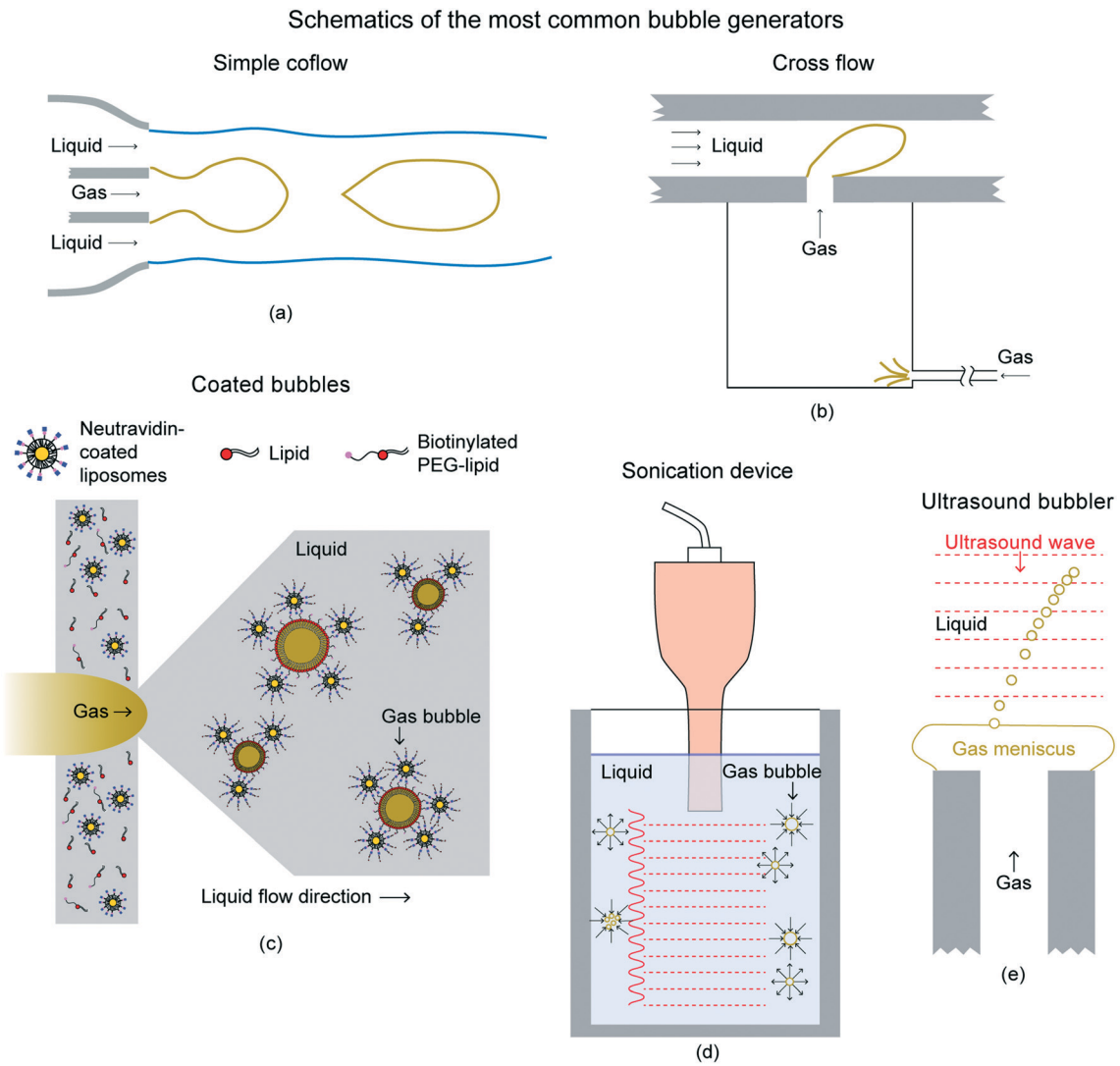

Fig. 7 Schematics of the most common bubble generators.[35] (a) Simple coflow configuration in which gas and liquid flow in the same direction. (b) Cross flow configuration in which the gas injected perpendicular to the liquid stream. (c) Creating shell for gas bubbles (d) sonicator inducing the growth and collapse of bubbles by means of an ultrasound field. (e) Ultrasound wave-driven generation of a train of monodisperse gas bubbles from a meniscus attached to the gas injector.

removed. In addition, similar mechanism is applied for other contaminants such as extremely fine particles or globules, which do not possess a significant settling rate.[14]

3.6 Surface cleaning

Gas bubbles can also be used as cleaning agents both for the prevention of surface fouling and for defouling of surfaces.[13,14] It has been observed that application of gas bubbles prevents the surfaces from fouling by inhibiting the adsorption of proteins onto various surfaces. The gas bubbles were generated electrochemically. Researchers investigated the effect of gas bubbles on bovine serum albumin (BSA) adsorption on mica surface by AFM imaging. They reported that gas bubbles can block BSA adsorption on mica surface, resulting in circular hollows on the BSA films. Thus, fouling prevention can be achieved by covering a surface with gas bubbles as they form a physical barrier against the adsorption of protein.

4 Generation of gas bubbles

There are various methods to create a gas bubble.[35] One of the simpler way to create a gas bubble is by using an injection device.[17–19] Examples of the injection devices include microsyringe, micropipette, and pipette. For an example, to create in-air gas bubble, the injection device's tip is dipped in the liquid, taken out, and gas is injected in till the gas bubble detaches from the tip. The type of gas injected will determine the type of gas enclosed by the gas bubble. The gas bubble volume can be controlled by the opening size of the injection device and the volume of gas injected. A smaller opening size will produce smaller gas bubbles and *vice versa*. As an example, for creating a soap + water solution's air bubble, injection devices with opening size on the order of 0.5–3 mm can produce the air bubbles of volume on the order of 10–1000 mm^3.[18,19] Similar way can be applied to create under-liquid gas bubbles. The injection device needs to be dipped in the liquid and gas needs to be injected. Once the gas bubble reaches a critical size, it detaches from the tip.

This method of generating gas bubbles creates problems when multiple gas bubbles have to be generated. This method may be lead to coalescing of consecutive gas bubbles.[35] Other ways of generating multiple gas bubbles are discussed in this section. Fig. 7 shows schematics of commonly used selected gas bubble generators.[35] Parameters including gas bubble size and frequency of producing gas bubbles can be controlled using these methods.

The simplest method to generate gas bubbles in a controlled manner, avoiding coalescence, consists of injecting the gas within a laminar liquid stream. In this technology, the liquid and gas flow rates are imposed independently, thus allowing for the separate control of the bubbling frequency and of the gas bubble diameter. The gas bubble generation techniques aided by an outer liquid flow field can be divided into two categories. The categories depend on whether the gas is supplied in the liquid direction, known as coflowing devices, or in a different one, known as cross-flow devices. In a coflow configuration, the liquid streamlines are parallel, as shown in Fig. 7(a). This configuration type can also be modified by constricting the outer flow. The flow-focusing geometry usually has advantages over the simple coflow device, as they decrease the gas bubble size and increase the generating frequency. This type of configuration can also be used to coat gas bubbles with substances such as lipids and liposomes, for biomedicine applications, as shown in Fig. 7(c). The coatings of substances, such as phospholipids, helps to prevent gas bubbles from coalescing or dissolving in the liquid. Cross-flow devices, *i.e.*, those in which the direction of the liquid stream is perpendicular to that of the gas are shown in Fig. 7(b). Cross-flow devices are also widely used to reduce gas bubble size and to increase the bubbling frequency.

Other techniques of generating gas bubbles are by using acoustic means. In the sound wave, the compression pulse promotes the growth of the gas cavity, whereas the rarefaction one forces the collapse and detachment of the gas bubble. One of the ways to achieve the same is by sonication, as shown in Fig. 7(d). The train of compression–rarefaction waves makes microscopic gas pockets first grow to macroscopic sizes and subsequently implode, generating a cloud of microbubbles and nanobubbles. This is also the central idea behind one of the most widely extended techniques presently employed to produce coated gas bubbles in medical practice. This procedure consists of inducing cavitation by acoustic means in a dissolution containing both the gas that will fill in the gas bubbles and the coating substance. Another way of using acoustic for creating gas bubbles is shown in Fig. 7(e). It uses an acoustic standing wave to induce the periodic formation and pinch-off of a cusp on the surface of a gas meniscus emerging from a needle, leading to a train of microbubbles that flow away from the tip.

5 Contact angle of gas bubbles on various surfaces

It is important to understand interaction of various gas bubbles with various surfaces because gas bubbles movement is dependent on the way a gas bubble interacts with a surface. The surface interaction is studied using a physical quantity called as contact angle (CA).[6] It the angle at which the bubble contacts a surface. A high gas bubble CA means the surface repels the gas bubble and low gas bubble CA means the surface attracts the gas bubble. A low gas bubble CA is more conducive for transport because the gas bubbles spreads over the surface.

The two types of gas bubbles are chosen: in-air gas bubble and under-liquid gas bubble. The chosen enclosed gas is air. The chosen liquid for in-air air bubbles is soap + water

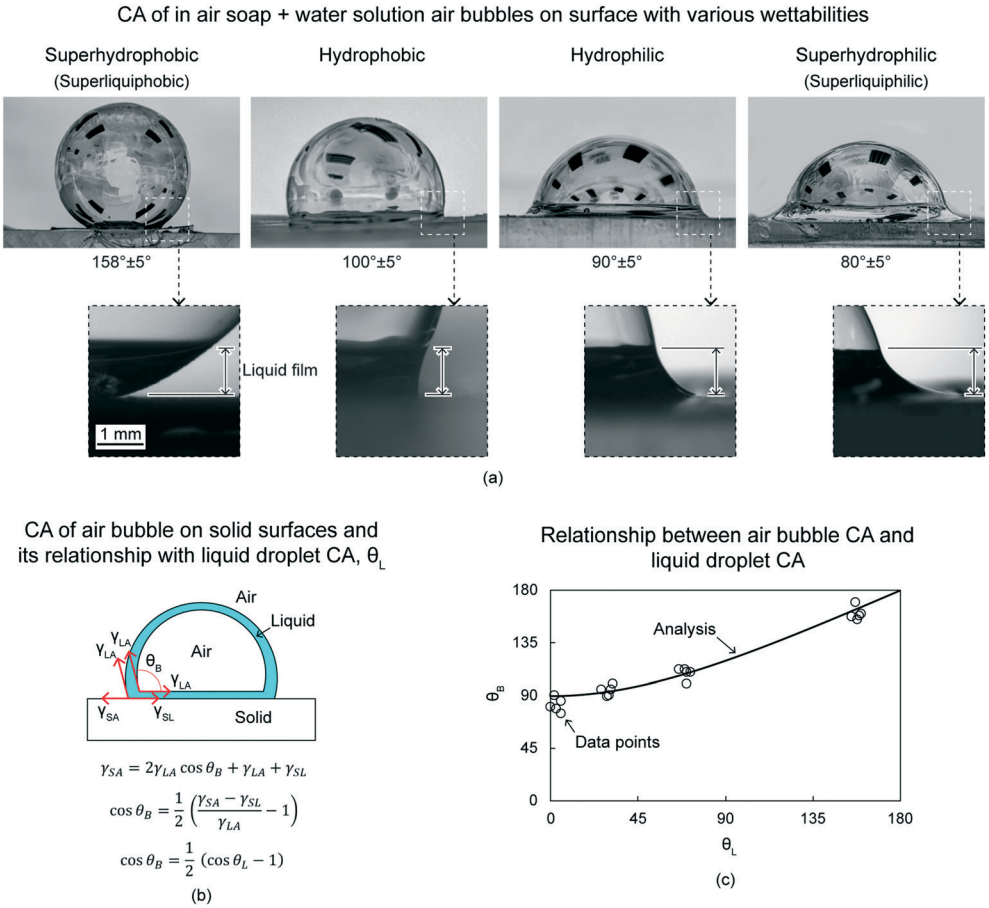

Fig. 8 (a) CA of in-air soap + water solution air bubbles on surfaces with various wettabilities (adapted from ref. 18). Various wettabilities include superhydrophobicity (superliquiphobicity), hydrophobicity, hydrophilicity, and superhydrophilicity (superliquiphilicity). Soap + water film is accumulated at the bottom (zoomed images), which forms different shapes on surfaces with various wettabilities. The typical height of the liquid film is ~1 mm. (b) Schematics of an air bubble on solid surface and its relationships with various surface tensions and liquid droplet CA (adapted from ref. 18). The CA of the air bubble and the liquid droplet are θ_B and θ_L, respectively. On a superhydrophilic surface, with θ_L = 0°, θ_B is 90°. (c) The data points are in agreement with the analytical relationship between θ_B and θ_L (adapted from ref. 18).

solution. The chosen liquids for under-liquid air bubbles are water, hexadecane, and soap + water solution.

5.1 Experimental method

This section describes various liquids used, fabrication of various wettabilities, and wettability characterization method.[18,19]

5.1.1 Liquids used. The liquids used were water, hexadecane, and soap + water solution.[18,19] The water used is distilled water. The hexadecane used is CAS number: 544-76-3 from Sigma-Aldrich. The soap + water solution used was prepared by mixing commercial dishwashing solution (Dawn Ultra, Procter & Gamble) and distilled water in an equal volume ratio. It was found that any lower ratio of soap to distilled water resulted in an unstable air bubble, lasting about 5 seconds.[18] This is because the thickness of an air bubble decreases with time due to the draining of the liquid surrounding the air bubble.[16] In addition, a pure soap + water solution has a short lifetime, about 10–20 seconds. Therefore, to further reduce the draining and increase the lifetime of an air bubble, about a 5% volume of glycerin (Dabur Glycerine Pure) was added. By adding glycerin, an air bubble lasted for about 5 minutes. More glycerin could be added for a further increase in stability.[16]

5.1.2 Various wettabilities. When the liquid CA is between 150° and 180°, 90° and 150°, 10° and 90°, or 0° and 10°, the surface is termed as superliquiphobic, liquiphobic, liquiphilic, or superliquiphilic surface, respectively.[6] These terms can be used for any liquid: water, hexadecane, or soap + water solution. If the discussion is about water specifically, then the term "–liqui–" changes to "–hydro–", resulting in superhydrophobic, hydrophobic, hydrophilic, and superhydrophilic, respectively.

Various surfaces chosen were with various wettabilities including superhydrophobicity, hydrophobicity, hydrophilicity, and superhydrophilicity.[18] The substrate chosen was an acrylic polymer, RGD720. The untreated acrylic polymer surface is hydrophilic. To achieve superhydrophilicity, the surface was treated under

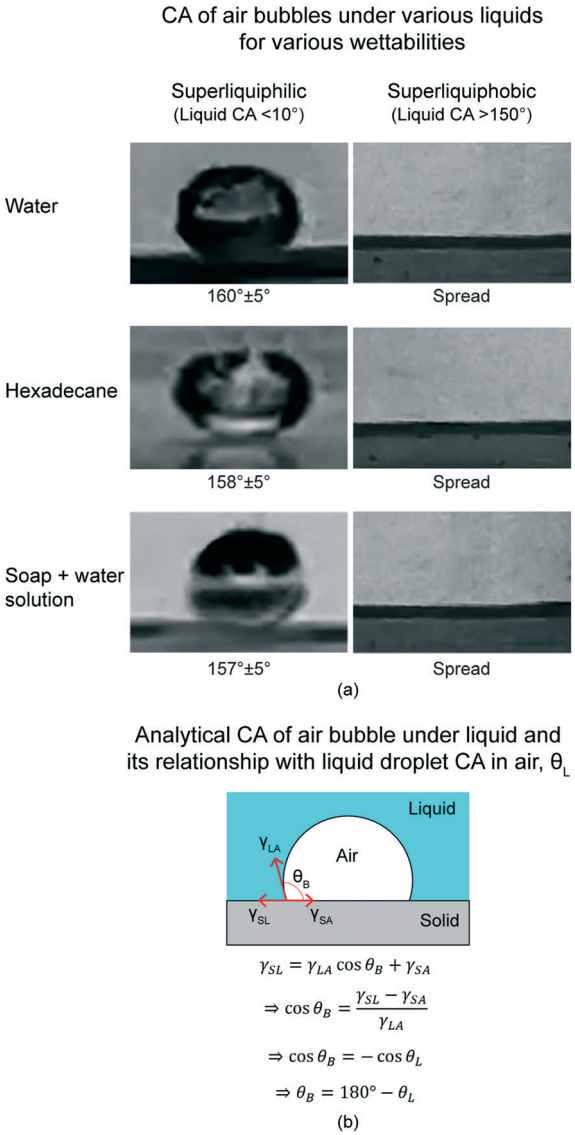

Fig. 9 (a) CA of air bubbles in various liquids for various wettabilities (adapted from ref. 19). Various liquids include water, hexadecane, and soap + water solution. Various wettabilities include superliquiphilicity and superliquiphobicity. Air bubbles have high CA on superliquiphilic surface, and it spreads completely on superliquiphobic surface, irrespective of the liquid. (b) Schematics of an air bubble in the liquid on a solid surface (adapted from ref. 19). The CA of the air bubble and liquid droplet are θ_B and θ_L, respectively. CA for both are related by $\theta_B = 180° - \theta_L$.

ultraviolet–ozone (UVO) light for 60 min. The UVO lamp used was a U-shaped lamp (18.4 W, Model G18T5VH-U, Atlantic Ultraviolet Co.), and the samples were kept directly underneath the light source. To achieve hydrophobicity, the untreated surface was coated with fluorosilane (448931, Sigma Aldrich) using vapor deposition. Samples were placed upside down and a droplet of fluorosilane was placed 1 cm below in an enclosure, which was left for 30 minutes.[6] Superhydrophobicity was introduced by spray coating a

Table 1 Physical properties of liquids used in this study

Liquid	Surface tension (mN m^{-1})	Density (kg m^{-3})
Water	72[a]	997[a]
Hexadecane	27[a]	770[a]
Soap + water solution (1 : 1 by volume)	30[b]	970[c]

[a] Ref. 38. [b] Ref. 39. [c] Ref. 19.

mixture of hydrophobic silica nanoparticles and binder on the uncoated surface.[6] Nanoparticles of size 7 nm (Aerosil RX300) and methylphenyl silicone binder (SR355S, Momentive Performance Materials) were used. The coating mixture was prepared by mixing 375 mg of the particles and 150 mg of the binder in 30 mL of solvent in an ultrasonifier (Branson Sonifier 450A, Emerson Electric Co., St. Louis, Missouri) for 30 minutes. The solvent used was 40% tetrahydrofuran (THF, Fisher Scientific) and 60% isopropyl alcohol (IPA, Fisher Scientific). Then the surface was UVO treated for 60 min and coated with fluorosilane, in the same fashion as described previously. This was done in order to achieve the superliquiphobicity of the hexadecane and the soap + water solution as well. In this review, the superhydrophobic and superhydrophilic surfaces can also be termed as superliquiphobic and superliquiphilic, respectively.

5.1.3 Wettability characterization. The wettability of the surfaces was characterized by measuring CA. The angles were measured using a standard automated goniometer (Model 290, Ramé-Hart Inc.). A microsyringe was used to deposit air bubbles and liquid droplets onto the surface, and a static

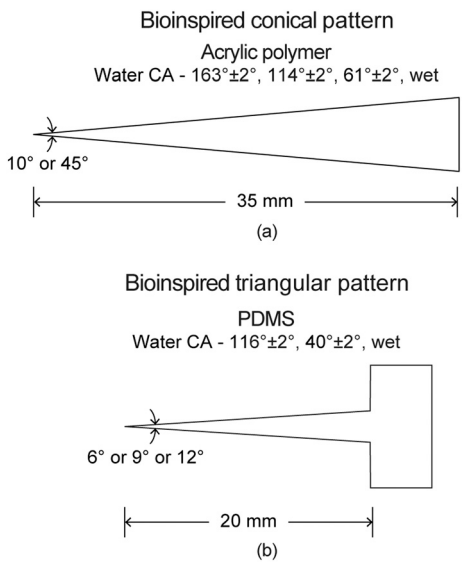

Fig. 10 Schematic of bioinspired (a) conical surface and (b) triangular pattern with a reservoir with various wettabilities (adapted from ref. 17 and 18).

profile image of the liquid–air interface was taken. The profile was analyzed using the DROPimage software in order to obtain CA. All angles were averaged over at least five measurements on different areas of the sample and reported as mean ± σ.

5.2 In-air air bubbles

This section presents CA of in-air air bubbles on various wettabilities. The liquid used is soap + water solution. The various wettabilities include superhydrophobicity, hydrophobicity, hydrophilicity, and superhydrophilicity. For this review paper, the superhydrophobic and superhydrophilic surfaces can also be termed as superliquiphobic and superliquiphilic, respectively.

Air bubble CA of superhydrophobic, hydrophobic, hydrophilic, and superhydrophilic surfaces are about 160°, 100°, 90°, and 80°, respectively. Fig. 8(a) shows optical images of the air bubbles on various wettabilities surfaces. As mentioned earlier, the boundary of a soap bubble drains with time, and the soap + water solution surrounds the air bubble near its bottom.[16] This forms a liquid film surrounding the air bubble. The zoomed optical images in Fig. 8(a), shows this liquid film and its thickness is about 1 mm. The figure also shows the liquid film's interaction with surfaces of various wettabilities. On the superhydrophobic surface, the liquid film is repelled by the surface. On the hydrophobic surface, the liquid film intersects almost perpendicular to the surface. On the hydrophilic surface, the liquid film wets the surface, and on the superhydrophilic surface, the liquid film wets the surface even more.

The air bubble CA can also be estimated analytically using various surface tensions and liquid droplet CA. Fig. 8(b) shows schematics of an air bubble. CA of an air bubble, θ_B, is given as

$$\cos\theta_B = \frac{1}{2}\left(\frac{\gamma_{SA}-\gamma_{SL}}{\gamma_{LA}} - 1\right) \quad (3)$$

where γ_{SA}, γ_{SL}, and γ_{LA} are solid–air, solid–liquid, and liquid–air surface tensions, respectively.[18,36] In which, the middle term relates with the liquid droplet CA, θ_L, which is given by Young's equation[6,37]

$$\frac{\gamma_{SA}-\gamma_{SL}}{\gamma_{LA}} = \cos\theta_L \quad (4)$$

Therefore, the relationship between θ_B and θ_L is given as

$$\cos\theta_B = \frac{1}{2}\left(\cos\theta_L - 1\right) \quad (5)$$

Graphical representation of this equation is shown in Fig. 8(c), where θ_B is plotted as a function of θ_L. The four data sets shown are of the superhydrophilic, hydrophilic, hydrophobic, and superhydrophobic surfaces. The shown analytical prediction is in agreement with the shown data points. It should be noted that θ_L ranges between 0–180°, and θ_B ranges between 90–180°.

In some cases, experimentally, it will appear that the air bubble CA is less than 90°.[18] Mathematically, that is when the ratio of the liquid film height, shown in Fig. 8(a), and the air bubble radius is high. However, it is to be noted that the liquid film is not underlying the air bubble, it is surrounding the air bubble near its bottom. Therefore, it does not affect the air bubble movement.

5.3 Under-liquid air bubbles

This section presents CA of under-liquid air bubbles on various wettabilities.[19] Various liquids are water, hexadecane,

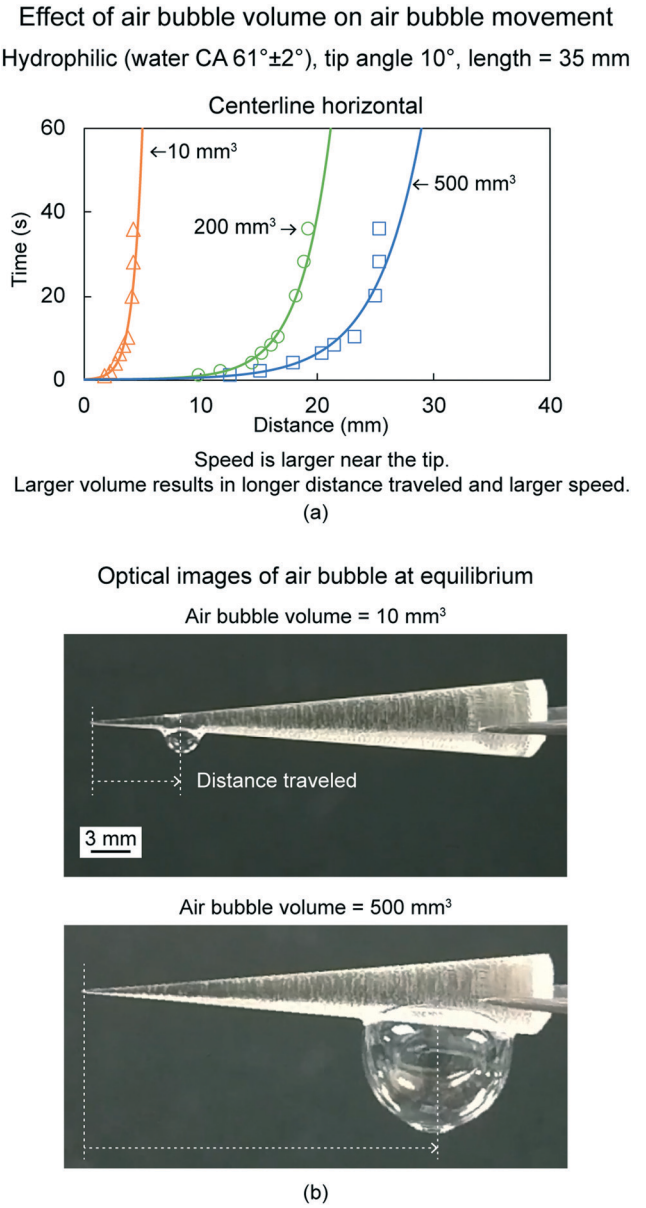

Fig. 11 (a) Effect of air bubble volume on air bubble movement (adapted from ref. 18). The distance traveled by an air bubble is shown as a function of time. (b) Optical images of air bubbles at equilibrium for two volumes at centerline horizontal orientations (adapted from ref. 18).

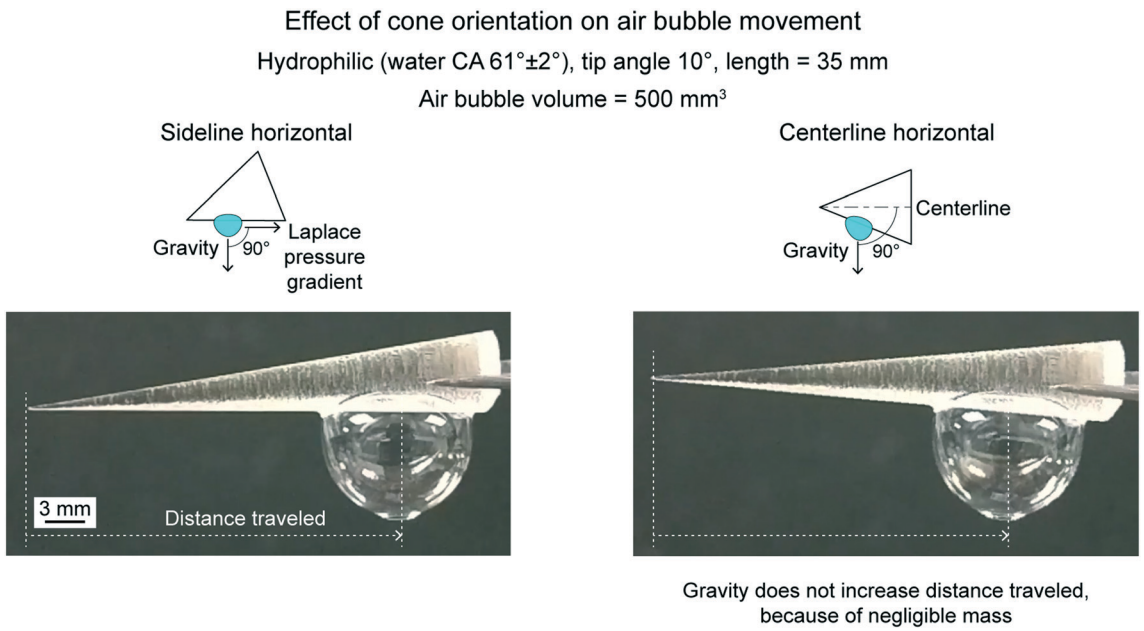

Fig. 12 Effect of cone orientation on air bubble movement with optical images of 500 mm^3 volume air bubbles at equilibrium at two cone orientations (adapted from ref. 18).

and soap + water solution. Various wettabilities are superliquiphobicity and superliquiphilicity.

Air bubbles CA of superliquiphilic are above 150° irrespective of the liquid used. Fig. 9(a) shows optical images of the air bubbles on surface with various wettabilities and various liquids. However, air bubbles will spread on the superliquiphobic surface irrespective of the liquid used. Exact opposite is observed in case of liquid droplets. Liquid droplets wet the superliquiphilic surface and form a CA of above 150° for the superliquiphobic surface.

These trends can be explained analytically by using different surface tensions. Fig. 9(b) shows schematics of an air bubble under liquid. CA of an air bubble under liquid, θ_B, is given as

$$\cos\theta_B = \frac{\gamma_{SL} - \gamma_{SA}}{\gamma_{LA}} \quad (6)$$

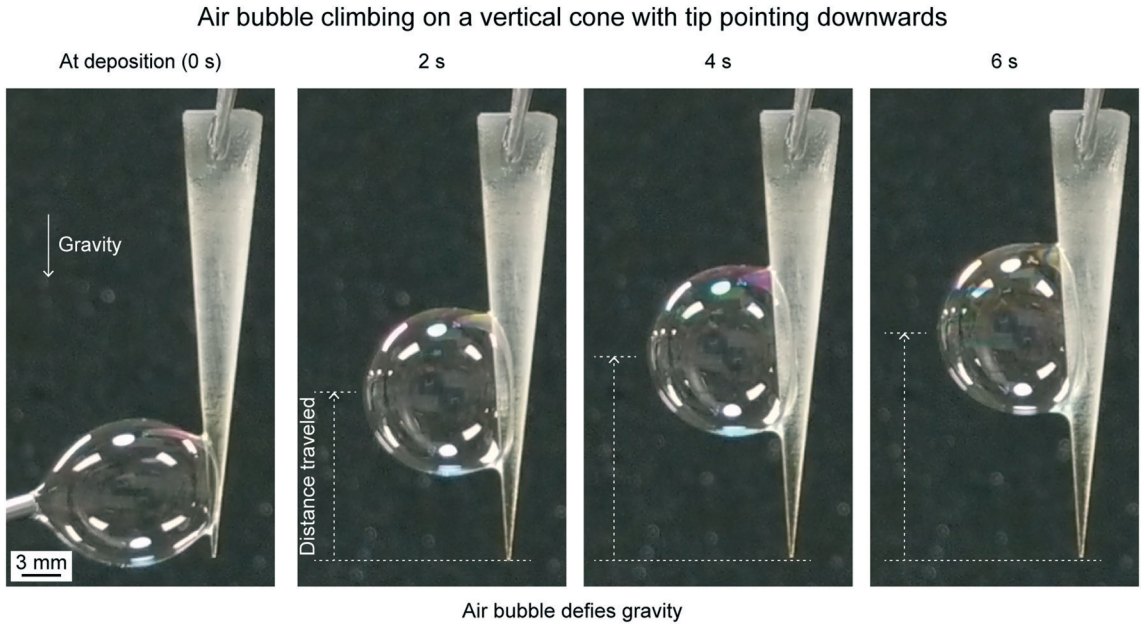

Fig. 13 Air bubble climbing on a vertical cone with the tip pointing downwards at different time intervals (adapted from ref. 18).

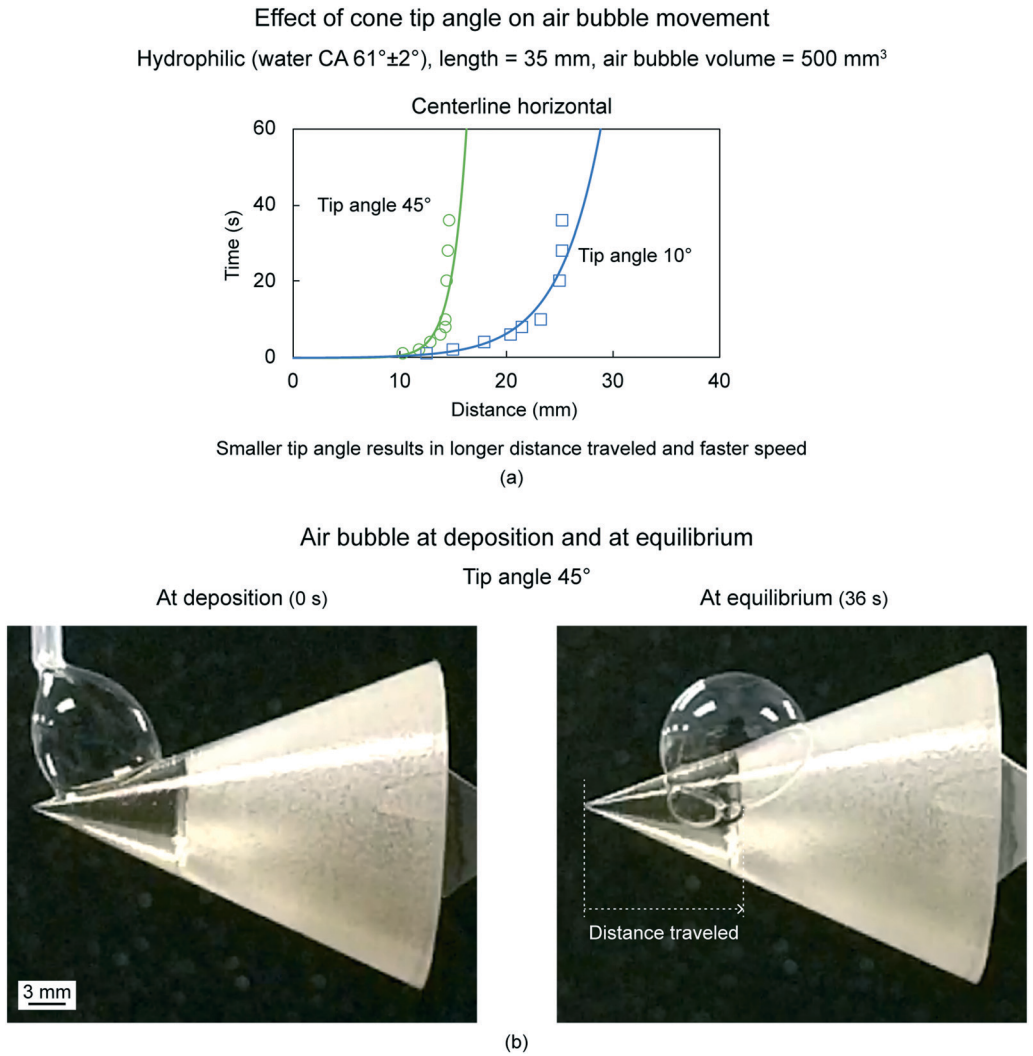

Fig. 14 (a) Effect of cone tip angle on the air bubble movement (adapted from ref. 18). The distance traveled by the air bubble is shown as a function of time. (b) Optical images of air bubbles at deposition and at equilibrium on the cone with tip angle 45° (adapted from ref. 18).

where γ_{SL}, γ_{SA}, and γ_{LA}, are solid–liquid, solid–air, and liquid–air surface tensions, respectively.[6,19,37] The right side of the expression is also given in eqn (4). Therefore, from eqn (4) and (6), the relation between θ_B and θ_L can be derived as[19]

$$\theta_B = 180° - \theta_L \quad (7)$$

This suggests that the air bubble CA under liquid and the liquid droplet CA in air are supplementary angles.

6 Bioinspired movement of gas bubbles

This section describes bioinspired methods for moving gas bubbles. The methods include using of bioinspired conical surfaces and triangular patterns. To evaluate the movement, controlled experiments were performed, in which single gas bubbles were placed at the cone's/triangle's tip and its distance travelled as a function of time were recorded. Both types of gas bubbles are described in this section: in air and under liquid. Effects of gas bubble volume, cone/triangle orientation, tip angle, and wettability were evaluated. For under-liquid gas bubbles effects of different liquids have also been evaluated. The chosen enclosed gas used here is air, therefore the term "air bubbles" is use throughout this section.

In this section, first, the experimental methods have been described. This is followed by description on movement study on in-air air bubbles. This includes air bubble movement using conical surfaces[18] and triangular patterns.[17] The in-air air bubble used is soap + water solution air bubble. Lastly, under-liquid air bubble movement using conical surfaces is described.[19] The liquids used are water, hexadecane, and soap + water solution. It was attempted to choose liquids with different surface tensions and densities, which are summarized in Table 1.

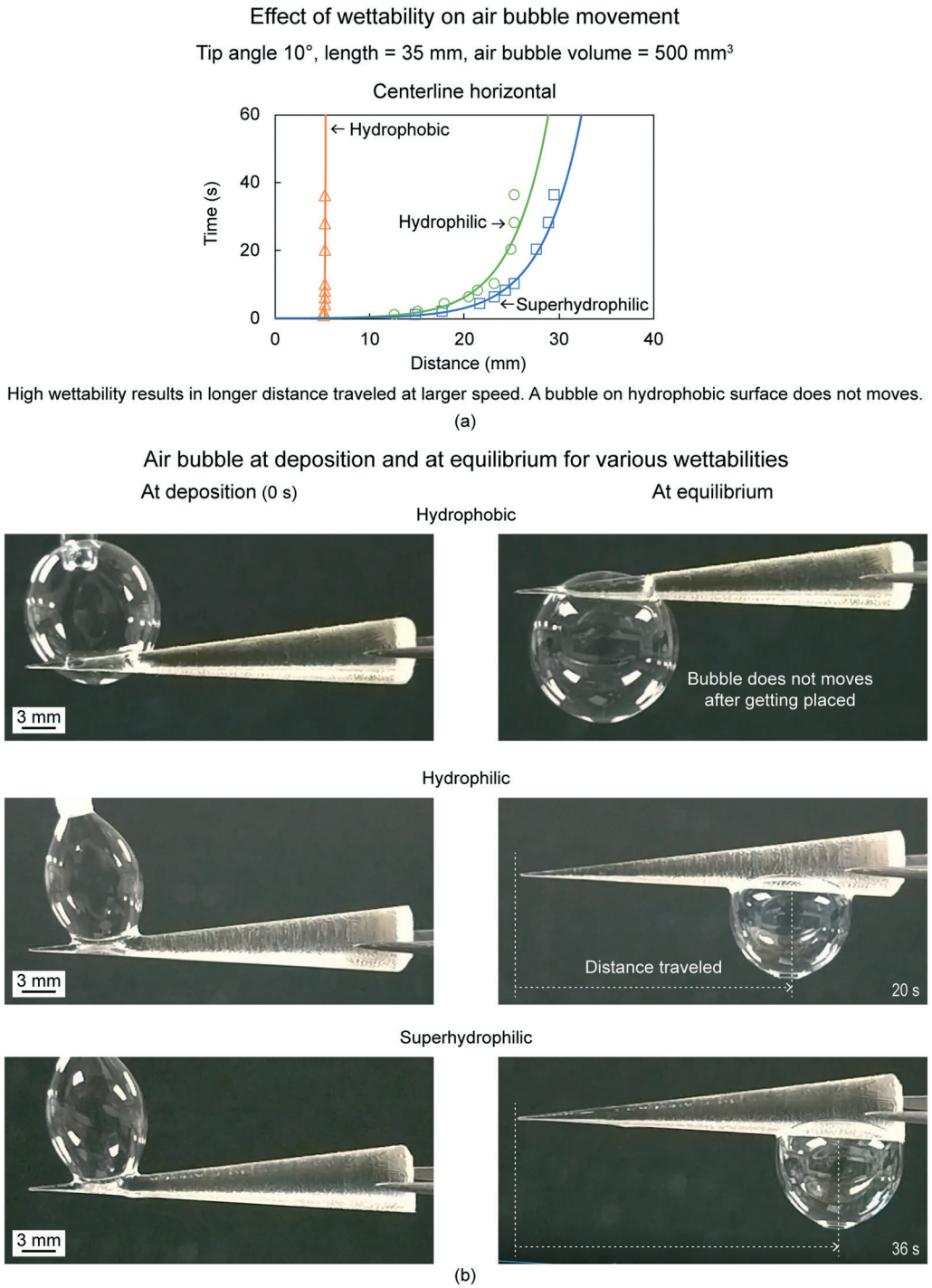

Fig. 15 (a) Effect of cone wettability on air bubble movement (adapted from ref. 18). The distance traveled by air bubbles is shown as a function of time. (b) Optical images of air bubbles at deposition and at equilibrium on cones with various wettabilities (adapted from ref. 18).

6.1 Experimental method

This section is divided into design, fabrication, various wettabilities, wettability characterization, various liquids used, and movement study.

6.1.1 Design. The conical shapes used to study the air bubble movement are inspired by cacti, whose conical spines have about a 10° tip angle.[6,20] Based on the authors' previous work, a representative cone length of 35 mm was chosen. For comparison, another cone with a higher tip angle of 45° and the same length was also chosen. Similarly, for the triangular pattern, tip angle of 9° was chosen. Based on the authors' previous work, a representative triangle length of 20 mm and a reservoir were chosen. For comparison, other triangular

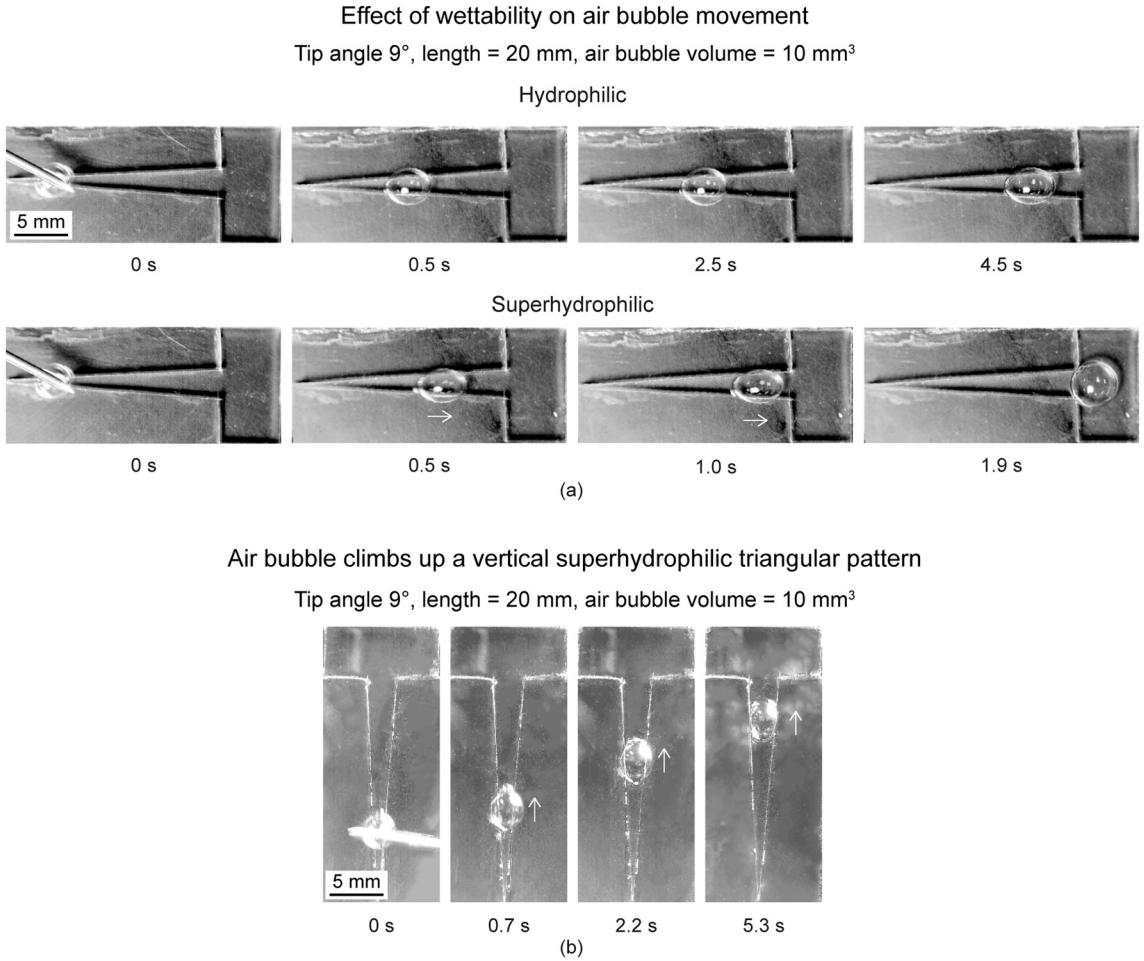

Fig. 16 (a) Selected photographs (top view) of the air bubbles transport at different times on hydrophilic and superhydrophilic triangular patterns with various wettabilities (adapted from ref. 17). (b) Air bubble climbs up a vertical superhydrophilic triangular pattern (adapted from ref. 17). Arrows shown represent air bubbles movement observed in videos.

patterns with different tip angle of 6° and 12° with the same length were also chosen. Fig. 10(a) and (b) show conical surfaces and triangular patterns used, respectively.

6.1.2 Fabrication. The cones were fabricated using additive manufacturing (3D printing) because it allows flexibility in designing and scalability. The machine used for 3D printing was Objet30 Prime, Stratasys, Ltd., Eden Prairie, Minnesota. It has an accuracy of about 0.1 mm. The material used was an acrylic polymer, RGD720.

The bioinspired triangular patterns were fabricated with polydimethylsiloxane (PDMS) coatings on a glass slide. In short, a glass slide was cleaned by acetone, isopropanol, and deionized water, and then dried by compressed air. After cleaning, a PDMS (Sylgard® 184, Dow Corning) coating was deposited on the glass slide. By removing air bubbles, curing, and cutting, a single triangular pattern was obtained.

6.1.3 Wettabilities. For the conical surfaces, four wettabilities were used which are superhydrophilic, hydrophilic, hydrophobic, and superhydrophobic. For triangular patterns, three wettabilities were used which are superhydrophilic, hydrophilic, and hydrophobic. Fig. 10(a) and (b) also show the wettabilities with water CA used for the conical surfaces and triangular patterns, respectively.

For the conical surfaces, the preparation of the four wettabilities have been discussed previously in section 5.1.2. Following is the brief description of the preparation again. The acrylic polymer is hydrophilic to begin with. It can be turned superhydrophilic by treated the untreated surface with UVO. To achieve hydrophobicity, the UVO treated surface was coated with fluorosilane. Superhydrophobicity was introduced by spray coating a mixture of hydrophobic silica nanoparticles and binder on the uncoated surface, and coating fluorosilane on top of it. Coating of fluorosilane was done to achieve the superliquiphobicity of hexadecane and the soap + water solution as well. In this review paper, the superhydrophobic and superhydrophilic surfaces can also be termed as superliquiphobic and superliquiphilic, respectively.

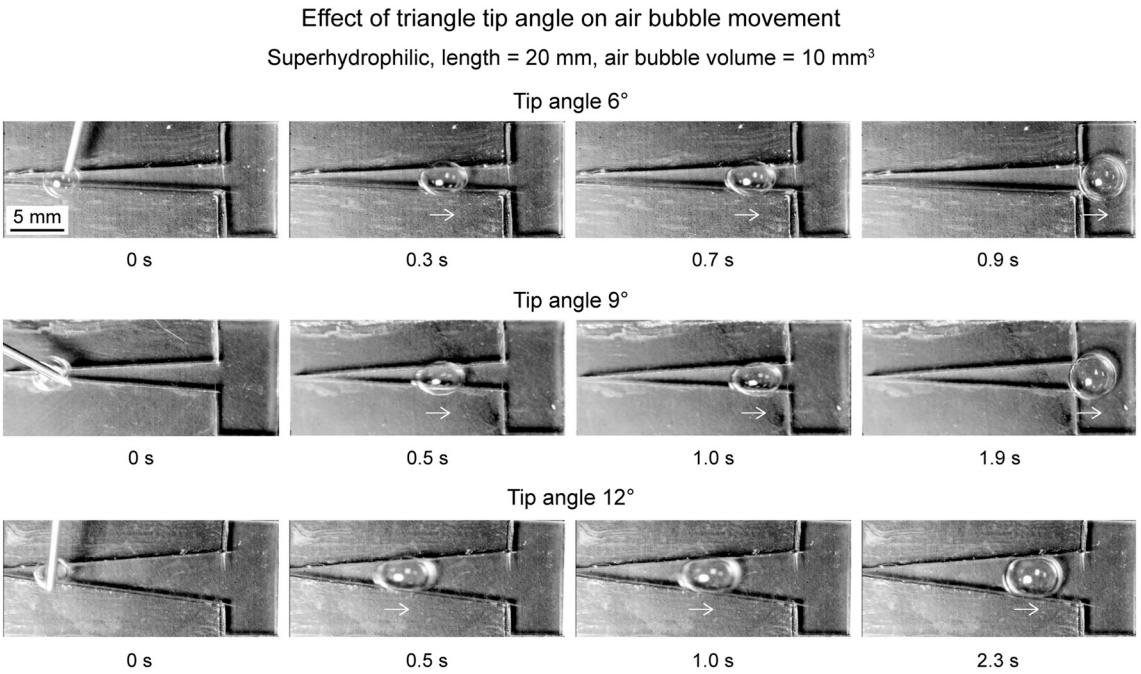

Fig. 17 Selected photographs (top view) of the air bubbles transport at different times on superhydrophilic triangular patterns with different tip angles (adapted from ref. 17). Arrows shown represent air bubbles movement observed in videos.

For triangular patterns, untreated PDMS substrate is hydrophobic. It was made hydrophilic or superhydrophilic by UVO treatment by using different treatment duration. Superhydrophilicity was achieved with longer UVO durations as compared to hydrophilicity.

6.1.4 Wettability characterization. The wettability characterization methods are the same for both conical surfaces and triangular patterns. The method has been discussed previously in section 5.1.3. To describe briefly, an injection device was use to place an air bubble on a flat surface and a static profile image of the liquid–air interface was taken. The profile was analyzed in a software to obtain CA. All angles were averaged over at least five measurements on different areas of the sample and reported as mean ± σ.

6.1.5 Liquids used. The preparation for the liquids have been discussed previously in section 5.1.1. Water and

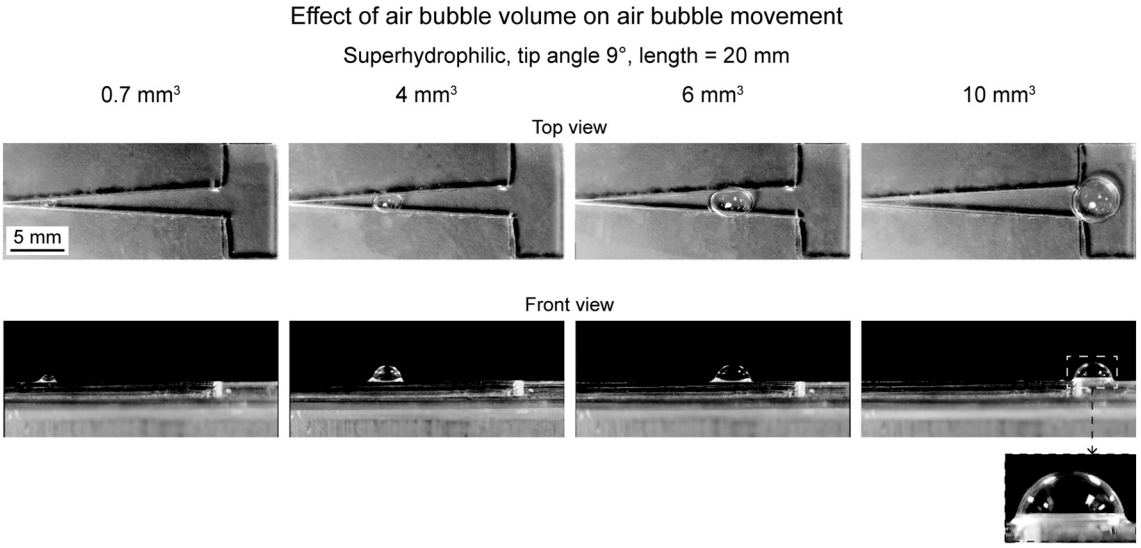

Fig. 18 Selected photographs (top and front view) of the air bubbles with different air bubble volume on superhydrophilic patterns at travel distances when the air bubbles stop (adapted from ref. 17).

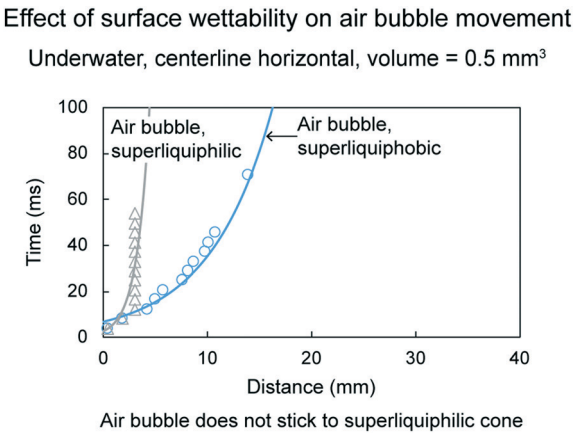

Fig. 19 Effect of surface wettability on air bubble movement (adapted from ref. 19). Distance traveled by air bubbles is shown as a function of time.

hexadecane were used as it is. Soap was mixed with water in equal volume ratio and about 5% glycerin by volume was added for high air bubble lifetime.

6.1.6 Movement study. Air bubble movement was studied by depositing an air bubble near the cone's or triangle's tip and recording its distance traveled with time. The distance was recorded from the tip of the cone to the center of the air bubble. For conical surfaces, the camera used was of Google Pixel 2, with 12 megapixels and a recording rate of 240 frames per second. For triangular patterns, the camera used was Koolertron, 5MP 20-300X. Effects of air bubble volume, cone/triangle orientation, tip angle, and wettability were evaluated. For under-liquid air bubbles effects of different liquids have also been evaluated.

The volume of an air bubble could be controlled by the opening size of the injection device and the volume of air injected. A smaller opening size will produce smaller air bubbles and *vice versa*. Therefore, injection devices including a microsyringe (Nordson, #7005005), a micropipette (USA Scientific, #1111-3800), and a pipette (Samco Scientific, #273) were used with an opening diameter of 0.5 mm, 1 mm, and 3

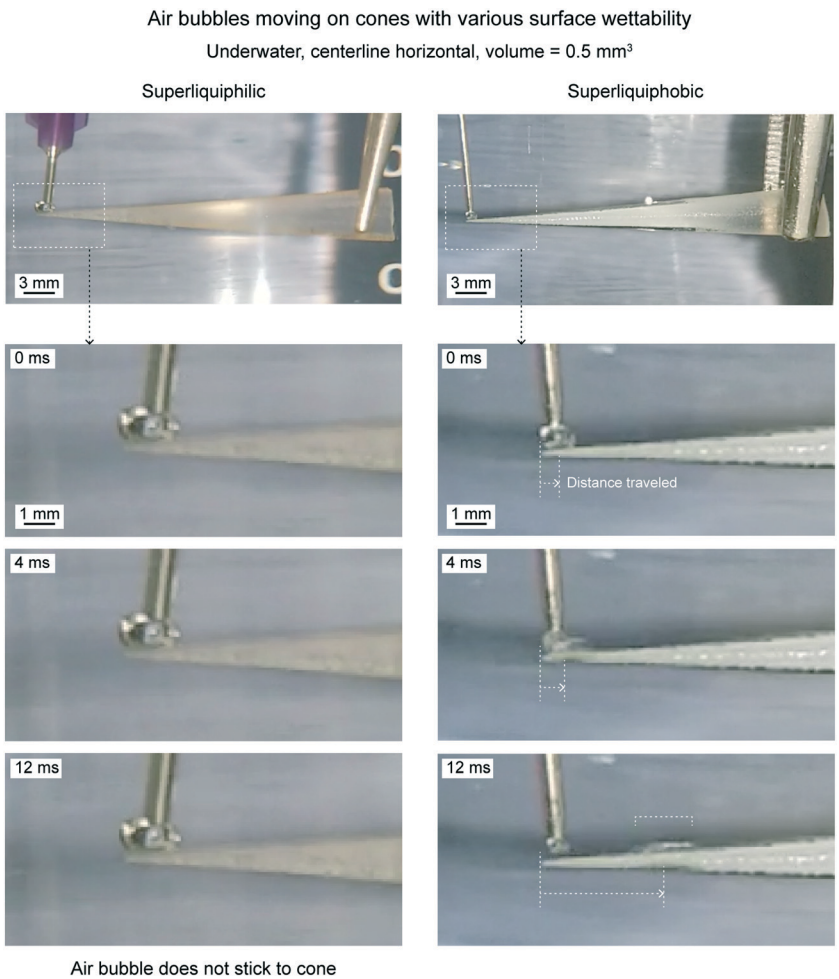

Fig. 20 Optical images of underwater air bubbles traveling on cones with various wettabilities (adapted from ref. 19).

mm, respectively. Different volumes of air bubbles used in these studies ranged from 0.5–1000 mm^3.

6.2 In-air air bubble

In this section, an overview of in-air air bubbles movement study on conical surfaces and triangular patterns is presented. The work was carried out by Gurera and Bhushan (2020)[18] and Feng and Bhushan (2020),[17] respectively. To evaluate the movement, single air bubbles were placed at the cone's/triangle's tip and its distance travelled as a function of time were recorded. The air bubble used is of soap + water solution.

6.2.1 Conical surfaces. For conical surfaces, effect of air bubble volume, cone orientation, tip angle, and cone wettability on the air bubble movements are presented.

6.2.1.1 Effect of volume. To evaluate effect of volume an untreated hydrophilic cone was chosen and movement of three volumes were studied including 10, 200, and 500 mm^3.[18] The cone orientation was chosen to be centerline horizontal, in which the centerline of the cone is parallel to the ground. Fig. 11(a) shows distance traveled by air bubbles as a function of time for the same. For any volume, an air bubble travels on a cone from tip to base.[18] This is because of the Laplace pressure gradient. The air bubble moves a certain distance and then stops. This is because the Laplace pressure gradient force decreases from tip to base, and it comes into equilibrium with the adhesion forces applied by the surface to the air bubble. This also implies that the speed of the air bubble is highest near the tip, and it decreases to zero as the air bubble moves along the cone length. An air bubble of higher volume moves to a longer distance with higher speed because the Laplace pressure gradient is directly proportional to the air bubble volume.[18,20] Fig. 11(b) shows optical images of two air bubbles of 10 mm^3 and 500 mm^3 volume at their equilibrium position after being placed. It is clear that a higher volume air bubble travels longer distance.

6.2.1.2 Effect of cone orientation. To evaluate effect of cone orientation an untreated hydrophilic cone, air bubble volume of 500 mm^3, and two orientations were chosen.[18] Fig. 12 shows the equilibrium position of the air bubbles and distance traveled by them, along with schematics of the two orientations. The cones were placed with either sideline or centerline horizontal orientation. Sideline horizontal orientation was used to study the role of Laplace pressure gradient on the movement of the air bubbles. Whereas, with centerline horizontal orientation, gravitational force also contributed to the movement. For both orientations, distance travelled by the air bubbles were similar. It is because, for centerline horizontal orientation, the gravity component driving the air bubbles is negligible, because of their negligible mass and low angle difference between the two orientations, being 5°.

To demonstrate that the Laplace pressure gradient can overcome gravity, an air bubble was placed on the tip of the cone pointing downwards as shown in Fig. 13. The air bubble climbed up and the distance traveled and speed attained by this air bubble were lower as compared to the centerline horizontal orientation.[18] This is because the effect of gravity working against the air bubble movement is at its maximum.

6.2.1.3 Effect of tip angle. To evaluate effect of cone tip angle, an untreated hydrophilic cone, air bubble volume of 500 mm^3, two tip angles, 10° and 45°, and cone orientation of centerline horizontal were chosen.[18] Fig. 14(a) shows the distance traveled by air bubbles as a function of time for the two tip angles. Fig. 14(b) shows air bubbles at deposition and at equilibrium on a cone of 45° tip angle. In a cone, with a tip angle, θ, and length, l, the radius is given by, $R = l\tan(\theta/2)$. The curvature gradient is higher in cones of smaller tip angle, hence, the Laplace pressure gradient is higher in cones of smaller tip angles. Therefore, a smaller tip angle results in longer distance traveled and faster speeds.

6.2.1.4 Effect of wettability. To evaluate effect of cone surface wettability, air bubble volume of 500 mm^3, cone tip angles of 10°, and cone orientation of centerline horizontal

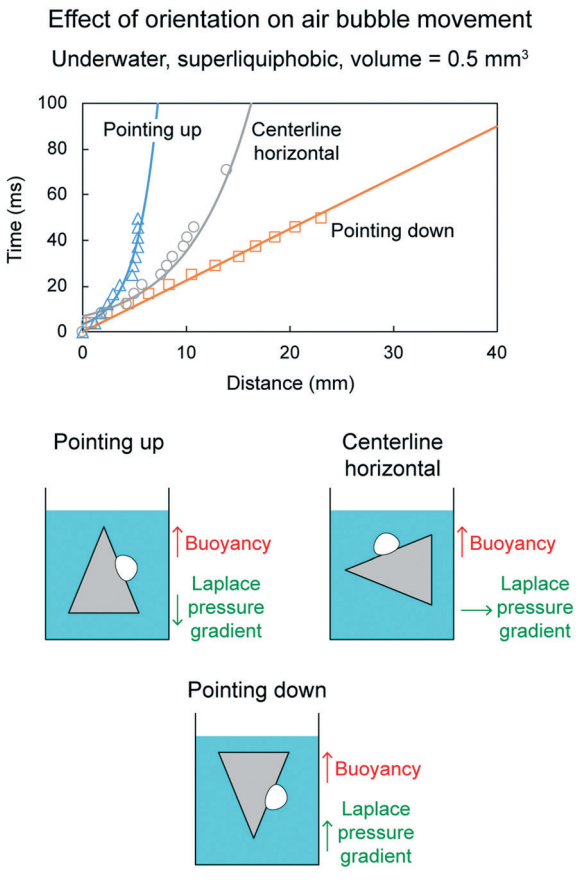

Fig. 21 Effect of cone orientation on air bubble movement (adapted from ref. 19). Distance traveled by air bubbles is shown as a function of time.

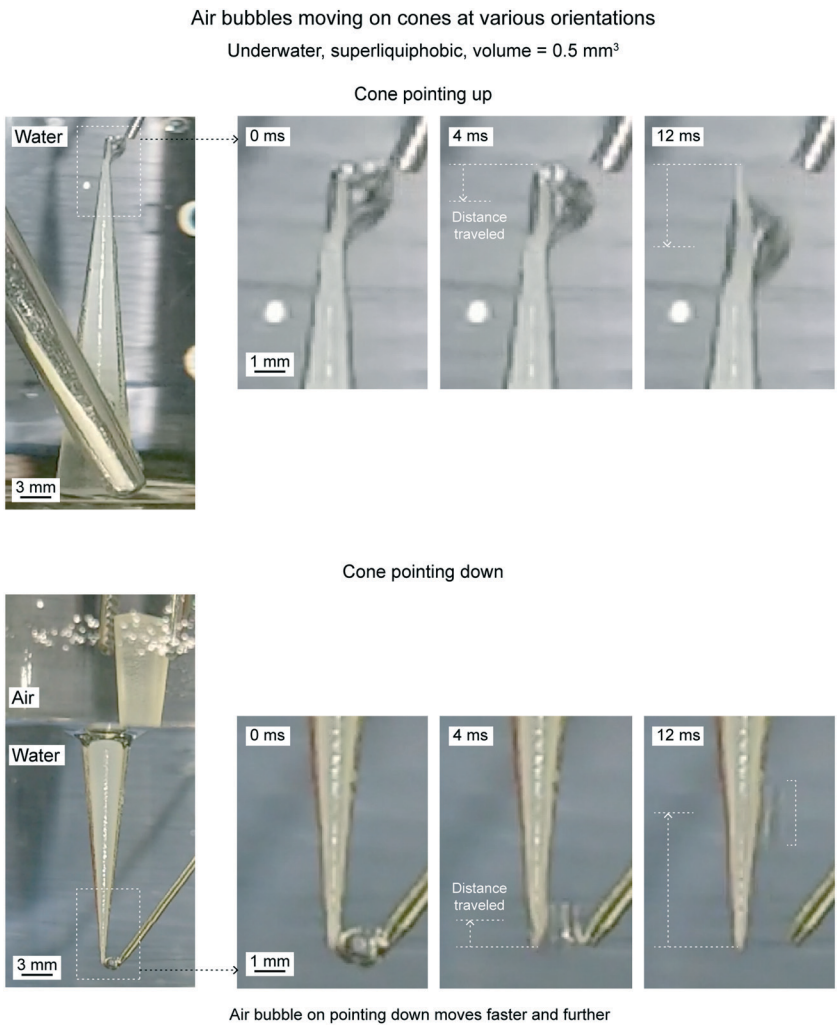

Fig. 22 Optical images of underwater air bubbles traveling on cones with various orientations (adapted from ref. 19).

were chosen.[18] Fig. 15(a) shows distance traveled by air bubbles as a function of time for three wettabilities, which include hydrophobicity, hydrophilicity, and superhydrophilicity. Fig. 15(b) shows air bubbles at deposition and at equilibrium on the cones for the three wettabilities. Air bubbles move only on hydrophilic and superhydrophilic cones. The air bubbles get stuck on the hydrophobic cone and do not move after being placed. This is because the liquid film surrounding an air bubble on the hydrophobic surface does not wet the surface, as shown in Fig. 8(a) (bottom). Higher wettability results in longer distance traveled at higher speed, this is because a higher wettability surface will be more wetted by the liquid film surrounding the air bubble.

6.2.2 Triangular patterns. For the triangular surfaces, effect of wettability and orientation, tip angle, and air bubble volume on the air bubble movement are discussed.[17]

6.2.2.1 Effect of wettability and orientation. To evaluate effect of wettability, triangle tip angle of 9° and air bubble volume of 10 mm^3 was chosen.[17] Various wettabilities evaluated were hydrophobicity, hydrophilicity, and superhydrophilicity. On the hydrophobic triangular pattern, when an air bubble is released, it stayed in the initial position where it was released and burst over time. For the other two wettabilities, the air bubbles moved to a distance and stopped. Fig. 16(a) shows movement of air bubbles on hydrophilic and superhydrophilic triangular. Selected optical images of air bubbles at different times are presented. Arrows shown below some air bubbles are based on air bubble movement observed in videos. On the hydrophilic triangular pattern, the air bubbles took about 4.5 s to move to certain distance. On the superhydrophilic triangular pattern, the air bubble reached the reservoir and took about 1.9 s for the complete movement. Therefore, higher wettability results in longer distance traveled at higher speed, this is because a higher wettability surface will be more wetted by the liquid film surrounding the air bubble.

To evaluate effect of orientation, a superhydrophilic triangular pattern was placed vertically with an inclination angle of 90°. Selected optical images of air bubbles on the

pattern sitting in the vertical direction are shown in Fig. 16(b). An air bubble could be transported spontaneously upward, defying gravity. Due to the presence of Laplace pressure gradient, the air bubble could overcome gravity and move upward. As expected, it took longer for the air bubble to reach the reservoir with the pattern sitting in the vertical direction. Superhydrophilicity played a key role in generating enough driving force to overcome gravitational forces. The surface of the liquid film with a significant curvature on a superhydrophilic pattern was more conducive to the transport of air bubbles than those deposited on the hydrophilic pattern.

6.2.2.2 Effect of tip angle. To evaluate effect of tip angle, triangle pattern with superhydrophilicity and air bubble volume of 10 mm^3 was chosen.[17] Various tip angles chosen were 6°, 9°, and 12°. It is understood that Laplace pressure inside an air bubble is inversely proportional to width of the triangle, from eqn (2). Therefore, it is expected that a lower tip triangle will create higher Laplace pressure gradient is the air bubble as it has lower rate of increase in width. This was also observed experimentally. Fig. 17 shows air bubbles movement on triangular patterns with various tip angles. An air bubble took 0.9 s to reach the reservoir on triangular pattern of tip angle 6°. Which is faster as compared to the air bubble on triangular pattern of tip angle 9°, which took about 1.9 s. The air bubble on triangular pattern of tip angle 12° took longer time but did not reach the reservoir. Therefore, a smaller tip angle results in longer distance traveled and faster speeds. In addition, as a general rule, for a gas bubble to move in a triangular pattern, the diameter of the air bubbles should be large enough to touch the boundary.

6.2.2.3 Effect of volume. To evaluate effect of air bubble, triangle pattern with superhydrophilicity and tip angle of 9° was chosen.[17] Various air bubble volume chosen were 0.7, 4, 6, and 10 mm^3. Fig. 18 shows movement of air bubbles for various volumes. The movement is shown from the top and side view. It is evident that the air bubble with higher volume moved to a longer distance. Only the air bubble with a volume of 10 mm^3 could reach the reservoir. Therefore, a higher volume air bubble travels longer distance.

6.3 Under-liquid air bubble: using conical surfaces

In this section, an overview of under-liquid air bubbles movement study on conical surfaces is presented. The work was carried out by Gurera and Bhushan (2021).[19] Effect of wettability, cone orientation, and liquids on the air bubble movements are presented.

6.3.1 Effect of wettability. Air bubble CA and liquid droplet CA are supplementary angles, as shown in Fig. 8(b). Therefore, the air bubble movement is expected to be more on surfaces with lower wettability. Fig. 19 shows the movement of air bubble at centerline horizontal orientation underwater. Both, superliquiphilic and superliquiphobic, surfaces were studied. As an example, volume for the air bubble was kept constant at 0.5 mm^3. Fig. 20 shows positions of air bubbles at different time intervals on superliquiphilic and superliquiphobic cone.

On a superliquiphilic cone, the underwater air bubbles typically do not stick to the cone tip. This is because a superliquiphilic cone is repellent to air bubbles. In rare cases, if an air bubble sticks, it will not move. It is believed, due to the spherical shape of the air bubble, there is not enough Laplace pressure gradient inside the air bubble to drive it. On a superliquiphobic surface, the air bubble spreads across the surface and reaches the base of the cone.

6.3.2 Effect of cone orientation. When an under-liquid air bubble is sitting on a cone, there are two forces acting on it. The force due to the Laplace pressure gradient and buoyancy force. The force due to the Laplace pressure gradient was discussed earlier. The buoyancy force, $F_{buoyancy}$, is given by

$$\rho V g \tag{8}$$

where ρ is density of the liquid, V is the volume of the air bubble, and g is the gravitational constant. The force due to the Laplace pressure gradient always drive the air bubble along the cone, irrespective of the cone orientation. However, depending on cone orientation, the buoyancy force can either drive, have insignificant effect, or oppose the air bubble movement along the cone. The direction of buoyancy force is always upwards. Therefore, both forces are driving the air bubble when the cone is pointing down. Only force due to the Laplace pressure gradient is driving the air bubble when the cone is in centerline horizontal orientation and the buoyancy force plays an insignificant role. When the cone is pointing upwards, the buoyancy force opposes the movement of the air bubble along the cone. Therefore, effect of orientation on air bubble movement needs to be studied.

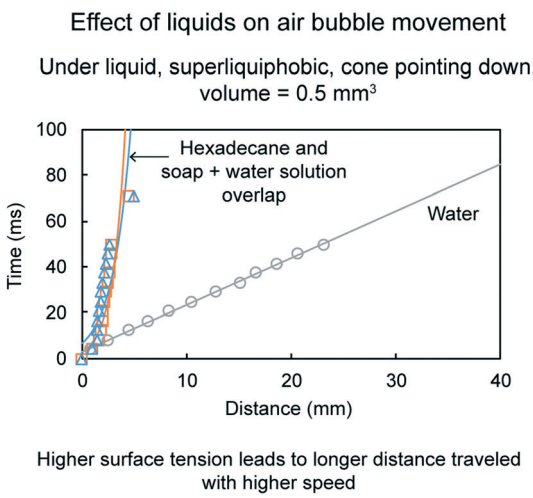

Fig. 23 Effect of liquids on air bubble movement (adapted from ref. 19). Distance traveled by air bubbles is shown as a function of time.

Fig. 21 shows distance traveled by air bubbles as a function of time, underwater on the superliquiphobic cone for 0.5 mm^3 volume at three different orientations, which are centerline horizontal, pointing up and pointing down. The three orientations are also shown schematically with the acting forces on the air bubble. Fig. 22 shows the position of an air bubble at different time intervals after being deposited on a cone pointing up and down orientations.

When the cone is pointing downwards, the air bubble travels farthest and fastest, as compared to all three orientations. It is because both the forces, the force due to Laplace pressure gradient and the buoyancy force, are acting upwards and drive the air bubbles. The air bubble travels nearest and slowest when the cone is pointing upwards. It is because both the forces act in the opposite direction. The buoyancy force opposes the movement.

6.3.3 Effect of liquid. The acting forces on air bubble, force due to the Laplace pressure gradient and buoyancy force, are a function of the surface tensions and density, respectively. Therefore, the effect of various liquids on the air bubbles movement needs to be studied. The chosen liquids were water, hexadecane, and soap + water solution. The chosen liquids were based on different surface tensions and densities of the liquids, which are summarized in Table 1.

Fig. 23 shows distance traveled by air bubbles as a function of time under various liquids on a superliquiphobic cone for 0.5 mm^3 volume at cone pointing down orientation. Fig. 24 shows the position of an air bubble at different time intervals after being deposited on cone pointing up for hexadecane and soap + water solution. As discussed before, when a cone is pointing downwards, two forces are driving the air bubble upwards, the Laplace pressure gradient and buoyancy force. As compared to water, hexadecane and soap + water solution have lower surface tensions. Therefore, the air bubble inside either of the liquids have lower Laplace

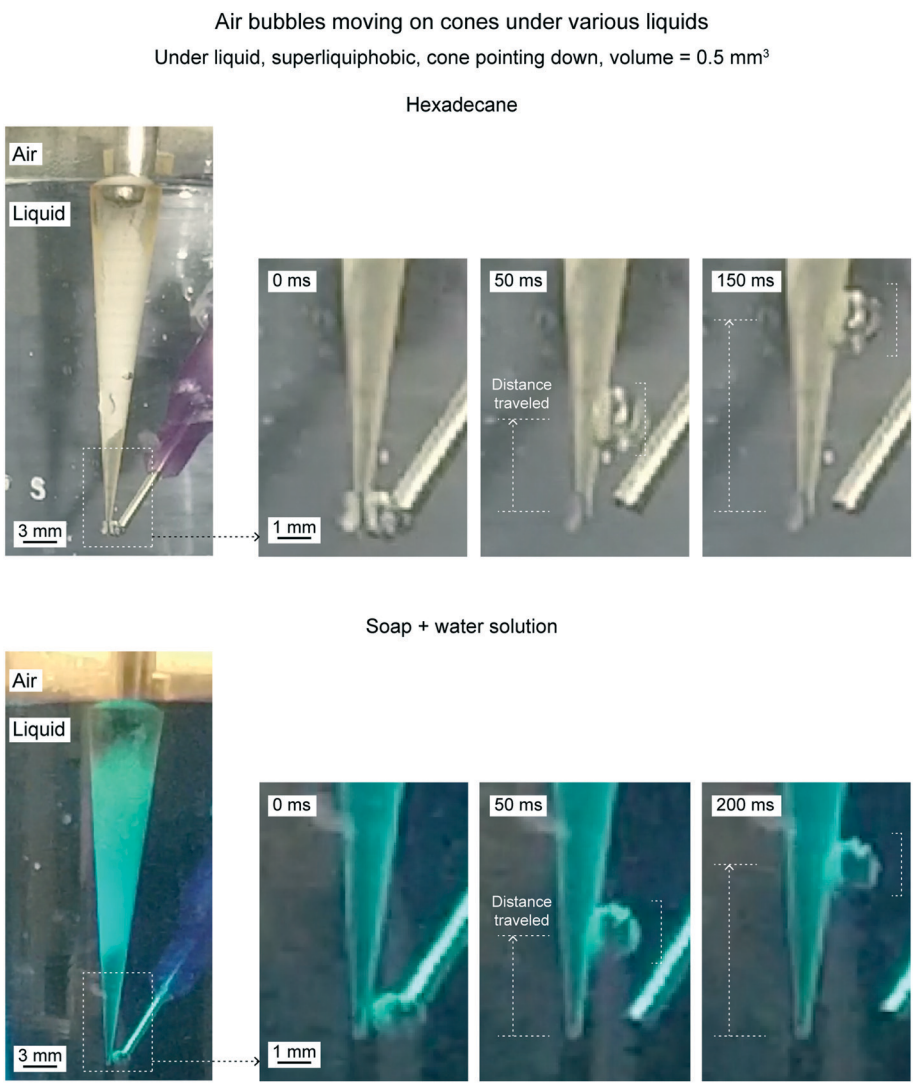

Fig. 24 Optical images of underwater air bubbles traveling on cones under various liquids (adapted from ref. 19).

pressure gradient, hence it travels slower than in water. For the chosen liquids the density did not play a deciding role. It is believed it was because the difference in densities did not turn out to be significant. A larger difference in densities could play a deciding role.

6.4 Outlook

In this section, gas bubbles movement was reviewed on bioinspired conical surfaces and triangular patterns. The gas studied was air and the liquid studied were water, hexadecane, and soap + water solution. Single air bubbles were placed at the tip and their movement were discussed. Both, in-air and under-liquid air bubbles were discussed. Effect of air bubble volume, orientation, tip angle, wettability, and liquid were also discussed. Based on the data, the following conclusions can be made. Conical surface and triangular patterns have the same qualitative conclusions. A large air bubble travels to long distance with large speed. For in-air air bubble, the conical surface/triangular pattern should be pointing upwards for better movement. Whereas for under-liquid air bubble, the conical surface/triangular pattern should be pointing downwards for better movement. A low tip angle increases the air bubble movement. High wettability improves the air bubble movement for in-air air bubbles, whereas the opposite is true for under-liquid air bubbles. For under-liquid air bubbles, high surface tension air bubbles move faster.

7 Conclusions

Gas bubbles are of interest in various applications including biomedicine, food production, drag reduction, water treatment, oil removal and surface cleaning. Therefore, studying gas bubbles movement in terms of their formation, interaction with underlying surfaces, and their movement is important. Bioinspired designs are proposed for moving gas bubbles including conical surfaces and triangular patterns. Both, conical surfaces and triangular patterns have the same qualitative performance. For an efficient conical surface/triangular pattern a low tip angle is desired, regardless the gas bubble type. For in-air gas bubble, the conical surface/triangular pattern should be pointing up with high wettability. For under-liquid gas bubble, the conical surface/triangular pattern should be pointing down with low wettability. For practical applications where gas bubbles collection is also a crucial part, then conical surfaces are deemed to be more applicable. It is because a bubble can come from any direction to get attached to the surface.

Conflicts of interest

There are no conflicts to declare.

References

1 J. R. Lindner, Microbubbles in medical imaging: current applications and future directions, *Nat. Rev. Drug Discovery*, 2004, **3**(6), 527–533.
2 S. Sirsi and M. Borden, Microbubble Compositions, Properties and Biomedical Applications, *Bubble Sci., Eng., Technol.*, 2009, **1**(1–2), 3–17.
3 S. P. Foam, *Engineering: Fundamentals and Applications*, Wiley, West Sussex, U. K., 2012, DOI: 10.1002/9781119954620.
4 H. Tsuge, *Micro-and Nanobubbles: Fundamentals and Applications*, CRC Press, Taylor & Francis Group, Boca Raton, Florida, 2014.
5 *Springer Handbook of Nanotechnology*, ed. B. Bhushan, Springer International, Cham, Switzerland, 4th edn, 2017, DOI: 10.1007/978-3-662-54357-3.
6 B. Bhushan, *Biomimetics: Bioinspired Hierarchical-Structured Surfaces for Green Science and Technology*, Springer International, Cham, Switzerland, 3rd edn, 2018 [cited 2018 Jun 16], (Biological and Medical Physics, Biomedical Engineering), Available from: www.springer.com/us/book/9783319716756.
7 E. C. Unger and T. O. Matsunaga, Lipid coated microbubbles and nanodroplets as tools for biomedical nanotechnology, in *Handbook of Materials for Nanomedicine*, ed. V. Torchilin and M. M. Amiji, Pan Stanford Publishing, Singapore, 2010 [cited 2020 Feb 7], pp. 749–786, Available from: https://arizona.pure.elsevier.com/en/publications/lipid-coated-microbubbles-and-nanodroplets-as-tools-for-biomedica.
8 S. Khasnavis, A. Jana, A. Roy, M. Mazumder, B. Bhushan and T. Wood, *et al.*, Suppression of Nuclear Factor-κB Activation and Inflammation in Microglia by Physically Modified Saline, *J. Biol. Chem.*, 2012, **287**(35), 29529–29542.
9 ed. G. F. Gutiérrez-Lopez, G. V. Barbosa-Cánovas, J. Welti-Chanes and E. Parada-Arias, *Food Engineering: Integrated Approaches*, Springer-Verlag, New York, 2008 [cited 2020 Jun 16], (Food Engineering Series), Available from: https://www.springer.com/us/book/9780387754291.
10 S. Deotale, S. Dutta, J. A. Moses, V. M. Balasubramaniam and C. Anandharamakrishnan, Foaming Characteristics of Beverages and Its Relevance to Food Processing, *Food Eng. Rev.*, 2020, **12**(2), 229–250.
11 S. L. Ceccio, Friction Drag Reduction of External Flows with Bubble and Gas Injection, *Annu. Rev. Fluid Mech.*, 2009, **42**(1), 183–203.
12 L. Wagenet, K. Mancl and M. Sailus, *Home Water Treatment (NRAES 48)*, Northeast Regional Agricultural Engineering Service (NRAES), Ithaca, New York, 1995 [cited 2020 May 13], Available from: https://ecommons.cornell.edu/handle/1813/67139.
13 Z. Wu, H. Chen, Y. Dong, H. Mao, J. Sun and S. Chen, *et al.*, Cleaning using nanobubbles: Defouling by electrochemical generation of bubbles, *J. Colloid Interface Sci.*, 2008, **328**(1), 10–14.

14 A. Gurung, O. Dahl and K. Jansson, The fundamental phenomena of nanobubbles and their behavior in wastewater treatment technologies, *Geosyst. Eng.*, 2016, **19**(3), 133–142.
15 B. Bhushan, *Introduction to Tribology*, Wiley, NY, 2nd edn, 2013, Available from: onlinelibrary.wiley.com/book/10.1002/9781118403259.
16 C. Isenberg, *The Science of soap films and soap bubbles*, Dover publications, Mineola, New York, 1992.
17 W. Feng and B. Bhushan, Spontaneous transport of air bubbles on bioinspired superhydrophilic triangular patterns, *J. Colloid Interface Sci.*, 2020, **575**, 399–405.
18 D. Gurera and B. Bhushan, Contact angles and movement of air bubbles on bioinspired conical surfaces, *J. Colloid Interface Sci.*, 2020, **577**, 530–541.
19 D. Gurera and B. Bhushan, Movement of air bubbles under various liquids using bioinspired conical surfaces, *J. Colloid Interface Sci.*, 2021, **582**, 41–50.
20 B. Bhushan, *Bioinspired Water Harvesting, Purification, and Oil-Water Separation*, Springer International, Cham, Switzerland, 2020 [cited 2020 Feb 6], (Springer Series in Materials Science), Available from: https://www.springer.com/gp/book/9783030421311.
21 C. Yu, M. Cao, Z. Dong, J. Wang, K. Li and L. Jiang, Spontaneous and Directional Transportation of Gas Bubbles on Superhydrophobic Cones, *Adv. Funct. Mater.*, 2016, **26**(19), 3236–3243.
22 B. Xu, Q. Wang, Q. Meng, M. He, C. Guo and L. Jiang, *et al.*, In-Air Bubble Phobicity and Bubble Philicity Depending on the Interfacial Air Cushion: Toward Bubbles Manipulation Using Superhydrophilic Substrates, *Adv. Funct. Mater.*, 2019, **29**, 1900487.
23 P. S. Brown and B. Bhushan, Bioinspired materials for water supply and management: water collection, water purification and separation of water from oil, *Philos. Trans. R. Soc., A*, 2016, **374**(2073), 20160135.
24 Y. Zheng, H. Bai, Z. Huang, X. Tian, F.-Q. Nie and Y. Zhao, *et al.*, Directional water collection on wetted spider silk, *Nature*, 2010, **463**(7281), 640–643.
25 B. Bhushan, Design of water harvesting towers and projections for water collection from fog and condensation, *Philos. Trans. R. Soc., A*, 2020, **378**(2167), 20190440.
26 É. Lorenceau and D. Quéré, Drops on a conical wire, *J. Fluid Mech.*, 2004, **510**, 29–45.
27 T.-Y. Wang, K. E. Wilson, S. Machtaler and J. K. Willmann, Ultrasound and Microbubble Guided Drug Delivery: Mechanistic Understanding and Clinical Implications, *Curr. Pharm. Biotechnol.*, 2014, **14**(8), 743–752.
28 P. S. Epstein and M. S. Plesset, On the Stability of Gas Bubbles in Liquid-Gas Solutions, *J. Chem. Phys.*, 1950, **18**(11), 1505–1509.
29 J. E. Chomas, P. Dayton, D. May and K. Ferrara, Threshold of fragmentation for ultrasonic contrast agents, *J. Biomed. Opt.*, 2001, **6**(2), 141–150.
30 M. J. K. Blomley, J. C. Cooke, E. C. Unger, M. J. Monaghan and D. O. Cosgrove, Microbubble contrast agents: a new era in ultrasound, *BMJ*, 2001, **322**(7296), 1222–1225.
31 Anonymous, Drinking Water Treatment – Aeration [Internet], Drinking Water and Human Health, 2020, [cited 2020 Jul 16], Available from: https://drinking-water.extension.org/drinking-water-treatment-aeration/.
32 P. L. Oakes, K. Gullett and T. Bobowick, Aeration of Ponds Used in Aquaculture [Internet], United States Department of Agriculture, 2011 Jul, [cited 2020 Jul 16], Report No.: AEN-3, Available from: https://directives.sc.egov.usda.gov/OpenNonWebContent.aspx?content=33946.wba#:~:text=The%20process%20of%20mixing%20air,light%20energy%20from%20the%20sun.
33 P. L. L. Walls, J. C. Bird and L. Bourouiba, Moving with Bubbles: A Review of the Interactions between Bubbles and the Microorganisms that Surround them, *Integr. Comp. Biol.*, 2014, **54**(6), 1014–1025.
34 Anonymous, Extracting impurities through the power of bubbles|A new dimension in water recycling|Environmental topics [Internet], Mitsubishi Electric Global Website, 2020 [cited 2020 Jul 16], Available from: https://www.mitsubishielectric.com/en/sustainability/environment/ecotopics/water/microbubbles/index.page.
35 J. Rodríguez-Rodríguez, A. Sevilla, C. Martínez-Bazán and J. M. Gordillo, Generation of Microbubbles with Applications to Industry and Medicine, *Annu. Rev. Fluid Mech.*, 2015, **47**(1), 405–429.
36 S. Arscott, Wetting of soap bubbles on hydrophilic, hydrophobic, and superhydrophobic surfaces, *Appl. Phys. Lett.*, 2013, **102**(25), 254103.
37 A. W. Adamson and A. P. Gast, *Physical Chemistry of Surfaces. sixth*, Wiley, New York, NY, 1997.
38 ed. J. R. Rumble, *CRC Handbook of Chemistry and Physics*, Taylor and Francis, Boca Raton, Florida, 100th edn, 2019, Available from: https://www.crcpress.com/CRC-Handbook-of-Chemistry-and-Physics-100th-Edition/Rumble/p/book/9781138367296.
39 P. L. Du Noüy, Surface Tension of Soap Solutions, *Nature*, 1932, **129**(3251), 278–279.